AD_____

Award Number: W81XWH-09-1-0459

TITLE: NF-kappaB Activity in Macrophages Determines Metastatic Potential of Breast Tumor Cells

PRINCIPAL INVESTIGATOR: Fiona Yull, Ph.D.

CONTRACTING ORGANIZATION: Vanderbilt University Medical Center
Nashville, TN 37203

REPORT DATE: August 2011

TYPE OF REPORT: Final

PREPARED FOR: U.S. Army Medical Research and Materiel Command
Fort Detrick, Maryland 21702-5012

REPORT DOCUMENTATION PAGE

Form Approved
OMB No. 0704-0188

1. REPORT DATE	2. REPORT TYPE	3. DATES COVERED
August 2011	Final	1 August 2009 -31 July 2011

4. TITLE AND SUBTITLE

NF-kappaB Activity in Macrophages Determines Metastatic Potential of Breast Tumor Cells

5a. CONTRACT NUMBER

5b. GRANT NUMBER
W81XWH-09-1-0459

5c. PROGRAM ELEMENT NUMBER

6. AUTHOR(S)

Fiona Yull

E-Mail: Fiona.Yull@vanderbilt.edu

5d. PROJECT NUMBER

5e. TASK NUMBER

5f. WORK UNIT NUMBER

7. PERFORMING ORGANIZATION NAME(S) AND ADDRESS(ES)

Vanderbilt University Medical Center
Nashville, TN 37203

8. PERFORMING ORGANIZATION REPORT NUMBER

9. SPONSORING / MONITORING AGENCY NAME(S) AND ADDRESS(ES)
U.S. Army Medical Research and Materiel Command
Fort Detrick, Maryland 21702-5012

10. SPONSOR/MONITOR'S ACRONYM(S)

11. SPONSOR/MONITOR'S REPORT NUMBER(S)

12. DISTRIBUTION / AVAILABILITY STATEMENT
Approved for Public Release; Distribution Unlimited

13. SUPPLEMENTARY NOTES

14. ABSTRACT

The contribution of NF-kappaB (NF-kB) signaling within macrophages to metastatic potential has not been directly investigated in vivo. We use novel transgenic models to address this question during breast to lung metastasis. Expression of an inhibitor (DN) or an activator (IKK) of NF-kB is induced by crossing either inducible transgenic with a second transgenic expressing the reverse transactivator (rtTA) protein in macrophages and administering doxycycline (dox) in drinking water. We have modulated NF-kB activity in macrophages to test effects on breast cancer metastasis to the lung. Using a tail vein model of metastasis we show that increased NF-kB activity in early stages of metastasis results in significant anti-tumor responses and that inhibition of NF-kB activity may have pro-tumor effects. Using the polyoma transgenic model of mammary tumorigenesis we have shown that inhibition of NF-kB may inhibit primary tumor progression. Our data suggest that NF-kB in macrophages influences metastatic potential of mammary tumor cells but that the timing of modulation of NF-kB activity in macrophages may be critical to potential therapeutic response.

15. SUBJECT TERMS
NF-kappaB, macrophages, doxycycline-inducible transgenes, metastasis

16. SECURITY CLASSIFICATION OF:			17. LIMITATION OF ABSTRACT	18. NUMBER OF PAGES	19a. NAME OF RESPONSIBLE PERSON
a. REPORT	b. ABSTRACT	c. THIS PAGE			USAMRMC
U	U	U	UU		19b. TELEPHONE NUMBER *(include area code)*

Table of Contents

	Page
Introduction……..…….	**4**
Body…….	**4**
Key Research Accomplishments…….…….	**12**
Reportable Outcomes……	**12**
Conclusion……	**14**
References……	**14**
Appendices……	**15**

INTRODUCTION

Both macrophages and NF-kappaB (NF-κB) signaling are known to be important in mammary tumorigenesis. However, the contribution of NF-κB signaling within the macrophages to metastatic potential has not been directly investigated *in vivo*. We proposed to use transgenic models in a novel combination to address this critically important question related to breast to lung metastasis. Expression of an inhibitor (DN) or an activator (IKK) of NF-κB can be induced by crossing either with a transgenic expressing the reverse transactivator (rtTA) protein in a specific cell type and administering doxycycline (dox) in drinking water (1). The rtTA protein has been targeted to macrophages (2). A third type of transgenics (NGL), act as an *in vivo* reporter of NF-κB activity and indicates overall inflammatory response (3). We have these transgenics and have combined them to modulate NF-κB activity in macrophages and to test the impact of this altered microenvironment on breast cancer metastasis to the lung. Our hypothesis was that NF-κB activity in macrophages determines metastatic potential and thus represents a target for inhibition of metastatic breast cancer. Many of the tumor-promoting mediators expressed by macrophages are under the transcriptional control of NF-κB. Elevated NF-κB activity is an integrator of inflammatory responses and is strongly correlated with tumors. An inflammatory microenvironment promotes increased metastasis. Therefore, it is likely that NF-κB activity within macrophages is a critical component of mammary metastasis, but this question had not been addressed directly. We designed a strategy to modulate NF-κB in macrophages *in vivo* and determine the impact of these changes on mammary to lung metastasis. When we commenced these studies we were expecting that increasing NF-κB in macrophages would skew them towards a pro-tumor tumor-associated macrophage (TAM) phenotype. We were predicting that these macrophages would induce a chronic inflammatory environment that would support tumor metastasis by increasing angiogenic and matrix remodeling signals. We proposed to address two questions. 1) Does activation of NF-κB in macrophages contribute to mammary metastasis? 2) Can inhibition of NF-κB in macrophages inhibit mammary to lung metastasis? Our original SOW described harvesting of animals and completing analysis after metastatic tumors had developed in the lungs. As the data from year 1 provided unexpected evidence suggesting a major effect at early stages of metastasis we amended the SOW to include investigation of events occurring during this early stage. As our results took us in an unexpected direction we requested a no cost extension of funding for the past year to complete studies that were necessary in order to publish these important findings.

BODY

Task 1. Determine effects of increased NF-κB activity in macrophages on mammary to lung metastasis:

Determine effects of increased NF-κB activity in macrophages on lung tumor development using a tail vein metastasis model.

These studies were designed to introduce breast tumor cells via the tail vein such that they metastasize to the lungs in mice in which we can inducibly activate NF-κB in macrophages. This is achieved by crossing homozygous c-fms-rtTA transgenics with heterozygous IKK transgenics to generate double IKFM transgenics plus c-fms-rtTA control littermates. When IKFM mice are treated with doxycycline (dox) provided at 2mg/ml in 5% sucrose drinking water *ad lib,* expression of the constitutive form of the IKK2 activator of NF-κB is targeted to macrophages. Experimental subsets include IKFM and control littermates for this and all following dox induction experiments. Polyoma-derived breast cancer cell lines were introduced via the tail vein into immunocompetent IKFM and control mice. Dox treatment started 1 week prior to cell injection and continued until harvest at 2 weeks (PY1) post cell injection. At the end point lungs were harvested and the total number of

visible lung metastases on the surface were counted. Our original hypothesis suggested that activation of NF-κB would have pro-tumor effects resulting in greater numbers of lung metastases. We were therefore surprised when our data showed the opposite effect with fewer metastases in IKFM mice as compared with control littermates (Figure 1). As this result was unexpected we repeated the study and obtained the same highly significant observation.

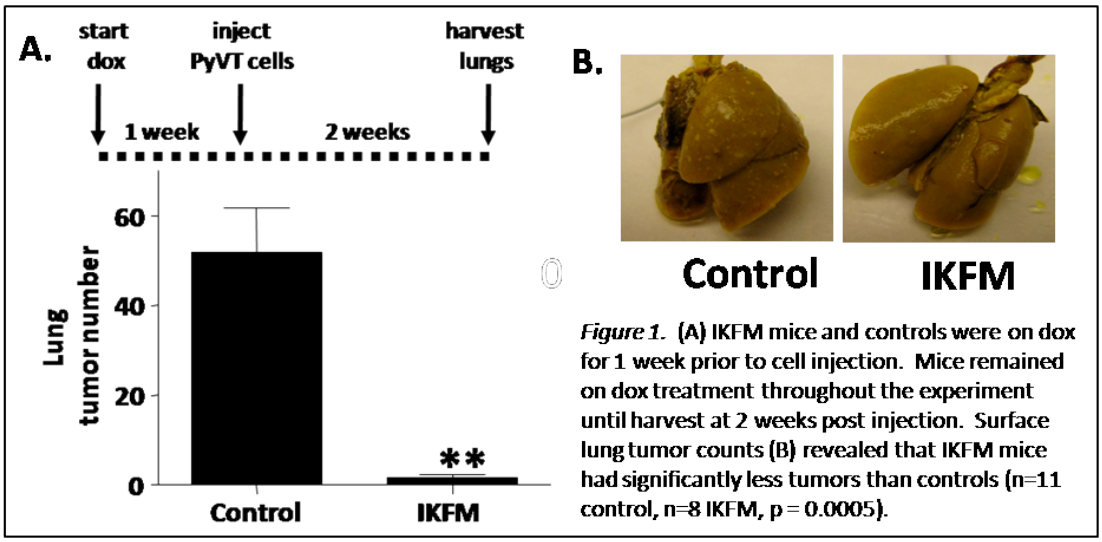

Figure 1. (A) IKFM mice and controls were on dox for 1 week prior to cell injection. Mice remained on dox treatment throughout the experiment until harvest at 2 weeks post injection. Surface lung tumor counts (B) revealed that IKFM mice had significantly less tumors than controls (n=11 control, n=8 IKFM, p = 0.0005).

*Determine effects of increased NF-κB activity in macrophages at **early stages** of metastasis on lung tumors using a tail vein metastasis model.*

Given the unexpected outcome of the studies above in which activation of NF-κB resulted in increased lung metastases we were interested to determine the results of our proposed studies in which we separated early versus later stages of metastasis. Polyoma cells were introduced via the tail vein with the same experimental strategy as above. To determine effects during early stages of metastasis dox treatment was started 1 week prior to cell injection and continued until 2 days post cell injection. Animals were sacrificed at 2 weeks (PY1) or 5 weeks (PY2) post cell injection. Lungs

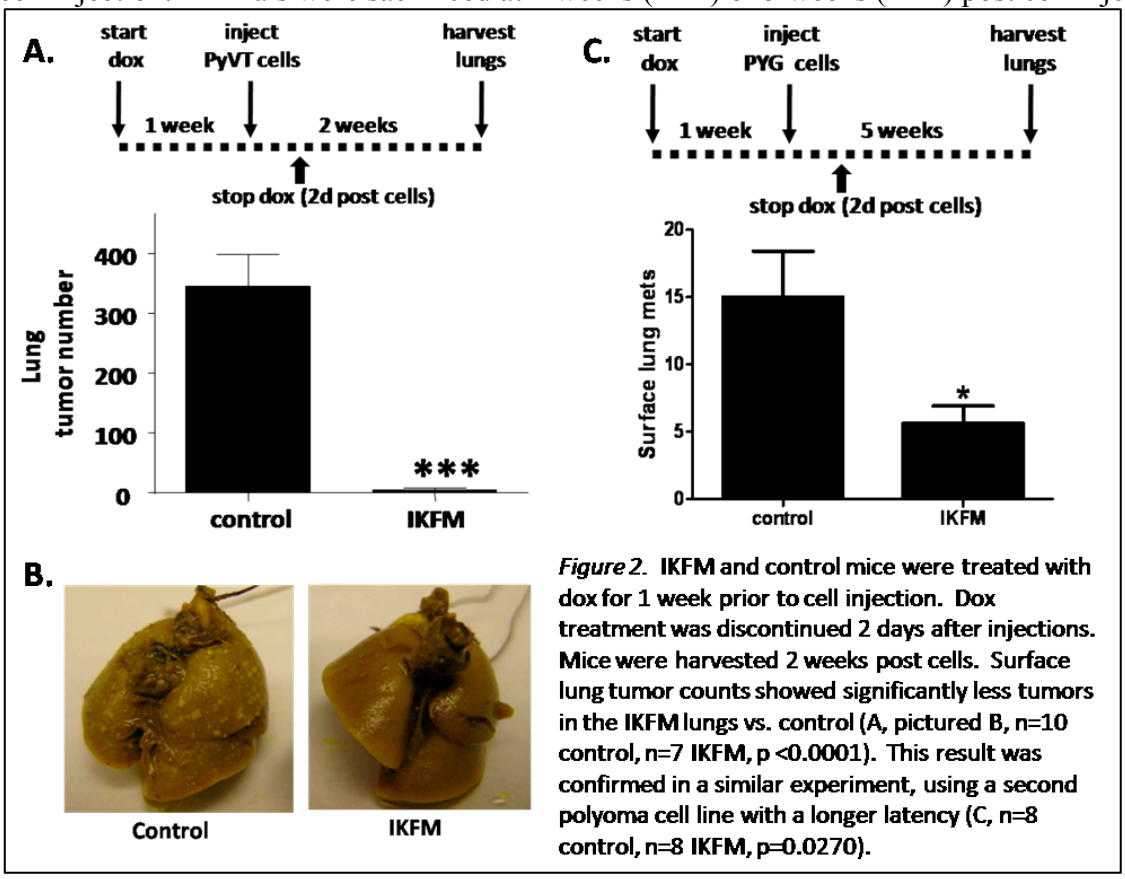

Figure 2. IKFM and control mice were treated with dox for 1 week prior to cell injection. Dox treatment was discontinued 2 days after injections. Mice were harvested 2 weeks post cells. Surface lung tumor counts showed significantly less tumors in the IKFM lungs vs. control (A, pictured B, n=10 control, n=7 IKFM, p <0.0001). This result was confirmed in a similar experiment, using a second polyoma cell line with a longer latency (C, n=8 control, n=8 IKFM, p=0.0270).

were harvested and lung metastases quantified. The data again show that increased NF-κB activity in the macrophages results in significantly fewer lung metastases (Figure 2). These results suggested that the anti-tumor effect of increased NF-κB activity was apparent very rapidly (within 2 days) after the cells were introduced via the tail vein.

*Determine effects of increased NF-κB activity in macrophages at **later stages** of metastasis on lung tumors using a tail vein metastasis model.* The data from the previous two studies demonstrated a strong anti-metastatic effect of increased NF-κB activity. However, our original hypothesis and recently published data from other groups (4-8) is suggestive that NF-κB activity in macrophages can be pro-tumor. The evidence that has been published has been obtained by investigation of tumor-associated macrophages (TAMs). We were thus interested to determine whether we would see this effect if the modulation of NF-κB activity was at a later stage during tumorigenesis when the behavior of the macrophages may be influenced by established metastatic tumors. PY1 or PY3 cells were introduced via the tail vein as above. Dox treatment was started at 2 days post injection. Animals were sacrificed and lungs harvested for quantification of lung metastases at 2 weeks. In these studies no significant impact on tumor numbers was observed (Figure 3).

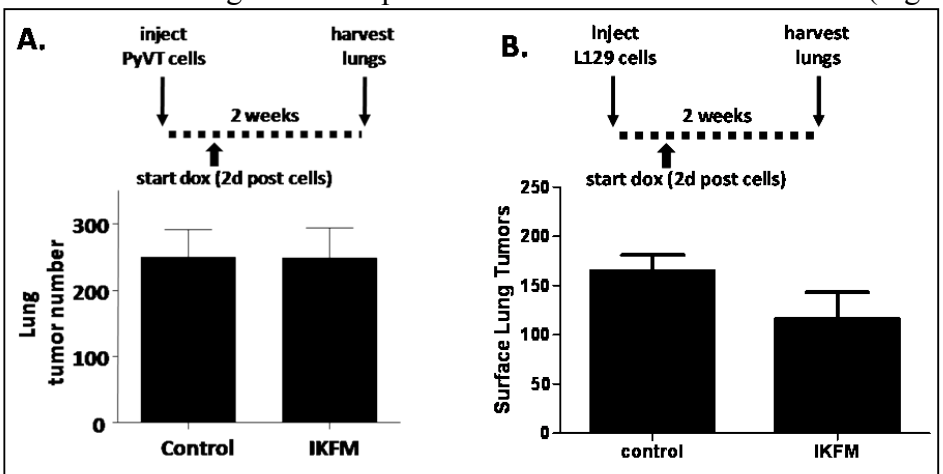

Figure 3. **IKFM mice and controls were injected with tumor cells at day 0. Two days post injection, dox treatment began and was continued until the time of sacrifice. Surface lung tumor counts (A) show that there was no significant difference between control and IKFM lung tumor burden (n= 7 control and n=6 IKFM, p =0.9859). This result was confirmed in a separate experiment (B), using a second polyoma cell line (n=10 control, n=11 IKFM, p=0.1540).**

This data suggests that at a very early stage in the metastatic process ie. 2 days post introduction of the tumor cells into the tail vein, the anti-metastatic effects of increased NF-κB activity in the macrophages are no longer effective. We were unable to detect any evidence of a pro-tumor effect in these studies. However, the tail vein injection methodology that we are using with introduction of relatively large numbers of aggressive tumor cells that rapidly result in large numbers of lung metastases may be too acute a model to observe pro-tumor effects. Given that different types of macrophages can have different functions we performed Flow analysis of cells harvested from lungs at this end point

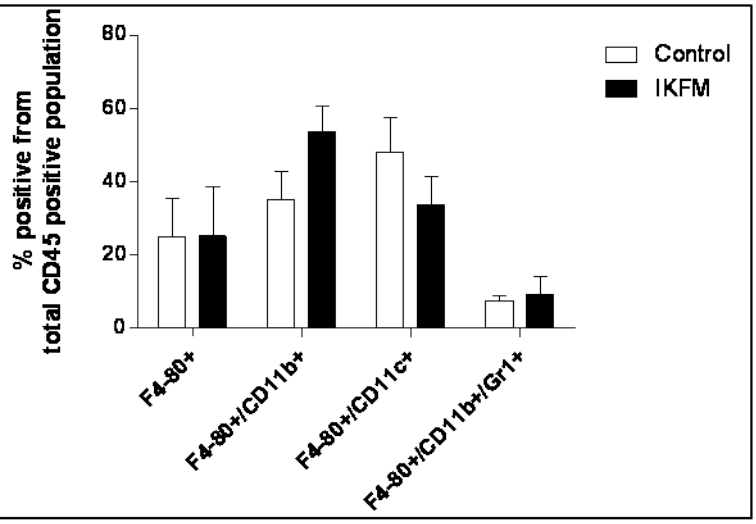

***Figure 4*. Flow data from IKFM mice and controls, injected with L129 cells. Dox treatment began two days post injection of cells and continued until time of sacrifice. Flow data reveals an elevated "recruited" macrophage phenotype in the IKFM lungs. (n=3 IKFM, n=3 control, p values not significant).**

(Figure 4). At this stage there is no change in the overall numbers of macrophages as defined using the antibody against F4/80. However, within the F4/80 positive population there is a trend towards an increase in the numbers of early stage F4/80/CD11b^{+} cells versus resident F4/80/CD11c^{+} populations. As no impact on tumor was observed during the later stages of metastasis we suspected that the changes in macrophage populations were probably greater at earlier stages in the process. It is likely that the macrophages that the tumor cells encounter when they are first injected have the greatest impact in this model.

To investigate the earlier effects on macrophage populations we performed flow cytometric analysis on lungs from control and IKFM mice after 1 week of dox treatment in the absence of cells, after 1 week of treatment followed by tail vein injection of tumor cells and harvest two days later and with dox treatment throughout until the final harvest at 2 weeks post tail vein introduction of cells. This analysis confirmed that increased NF-κB activity in the macrophages of IKFM mice results in early changes in macrophage populations in the lung with an increase in early stage versus mature macrophage populations (Figure 4 Connelly *et al*, 2011 – appended).

As M1 phenotype macrophages are considered as anti-tumor and M2 as pro-tumor we used quantitative real-time PCR analysis to investigate expression patterns of M1 versus M2 markers in lung homogenates from IKFM and control mice treated with dox for 1 week. The results suggest that the majority of cells may have shifted towards an M1 phenotype as M1 markers are increased and M2 are decreased (Figure 5 Connelly *et al* 2011).

To determine whether the tumor cells were reaching the lungs following tail vein injection or were being deleted rapidly in the blood we treated IKFM mice and controls with dox for 1 week, introduced tumor cells and prepared RNA from whole lung samples at 1 hour and 6 hours post injection. Quantitative real time PCR analysis of polyoma expression confirmed that cells were successfully reaching the lungs at 1 hour in IKFM mice but were significantly depleted by 6 hours. This suggested that the tumor cells may be being rapidly killed upon reaching the lungs. Using western analysis for cleaved caspase-3 we show that there is no measurable cleaved caspase-3 in the absence of tumor cells, or in control mice at 6 hours following introduction of tumor cells but there is a significant increase in cleaved caspase-3 at 6 hours in IKFM lungs. This suggests that tumor cells are dying rapidly in this environment. To begin to address the mechanism by which this happens we measured reactive oxygen species and determined that these are significantly increased in IKFM lungs. To further investigate the lung environment at the time of tumor injection, cytokine profiling of bronchial alveolar lavage fluid from IKFM mice and controls after 1 week dox was performed using an R&D Systems Proteome Profiler mouse cytokine panel array kit. The only significant difference detected was an increase in levels of CXCL9 (MIG) and this was confirmed using real-time PCR analysis on lung mRNA (Figure 6 Connelly *et al* 2011).

Our data suggests that increased NF-κB signaling in macrophages induces a hostile environment for tumor cell seeding within the lungs. However, to determine the mechanisms leading to the observed phenotype it will be important to determine what genes are being up or down regulated specifically within the CD11b+ve cell population in the lungs of IKFM mice: the population which is expressing the cIKK2 transgene and driving the changes within the lung. Therefore, we isolated CD11b+ve cells from the lungs of IKFM and control mice treated with dox for one week. Upon initial real time analysis of these samples for up-regulation of "expected" NF-κB targets, such as TNF-α and Cox-2, we found no significant up-regulation within the macrophages themselves. We determined to run microarray analysis of n=1 control and n=1 IKFM CD11b +ve cell samples as an indicator of which targets are being affected. GeneChip Mouse Gene 1.0 ST whole transcriptome arrays (Affymetrix) were used to probe for the expression of 28,853 mouse genes. The array procedure was performed by the Vanderbilt Genome Sciences Resource. Preliminary analysis shows differential expression of over 2000 transcripts (at least 2 fold change, IKFM over control). At the top of the list, among the most up-regulated genes in the IKFM CD11b+ve cell sample are those recognized as "interferon-induced," such as Iigp1 (interferon inducible GTPase1) and Gbp1 (interferon induced guanylate binding protein). Additionally, as our transgene specifically up-regulates NF-κB signaling, we also probed the microarray data for genes

that were both up-regulated in the CD11b+ve cells of IKFM mice and were known NF-κB targets. Genes meeting this criteria include CXCL9, CXCL10, Gbp-1, CCR5, FAS, thrombospondin-1, HIF-1α, IRF-1, IRF-7, and others. From this list, four targets have been further validated in a full set of samples via real-time PCR, and we have confirmed their up-regulation within the CD11b+ve cells of IKFM mice (Figure 5). Each of these targets could be playing a role in the phenotype we have observed within the IKFM lungs, as most of them are associated with "anti-tumor" responses.

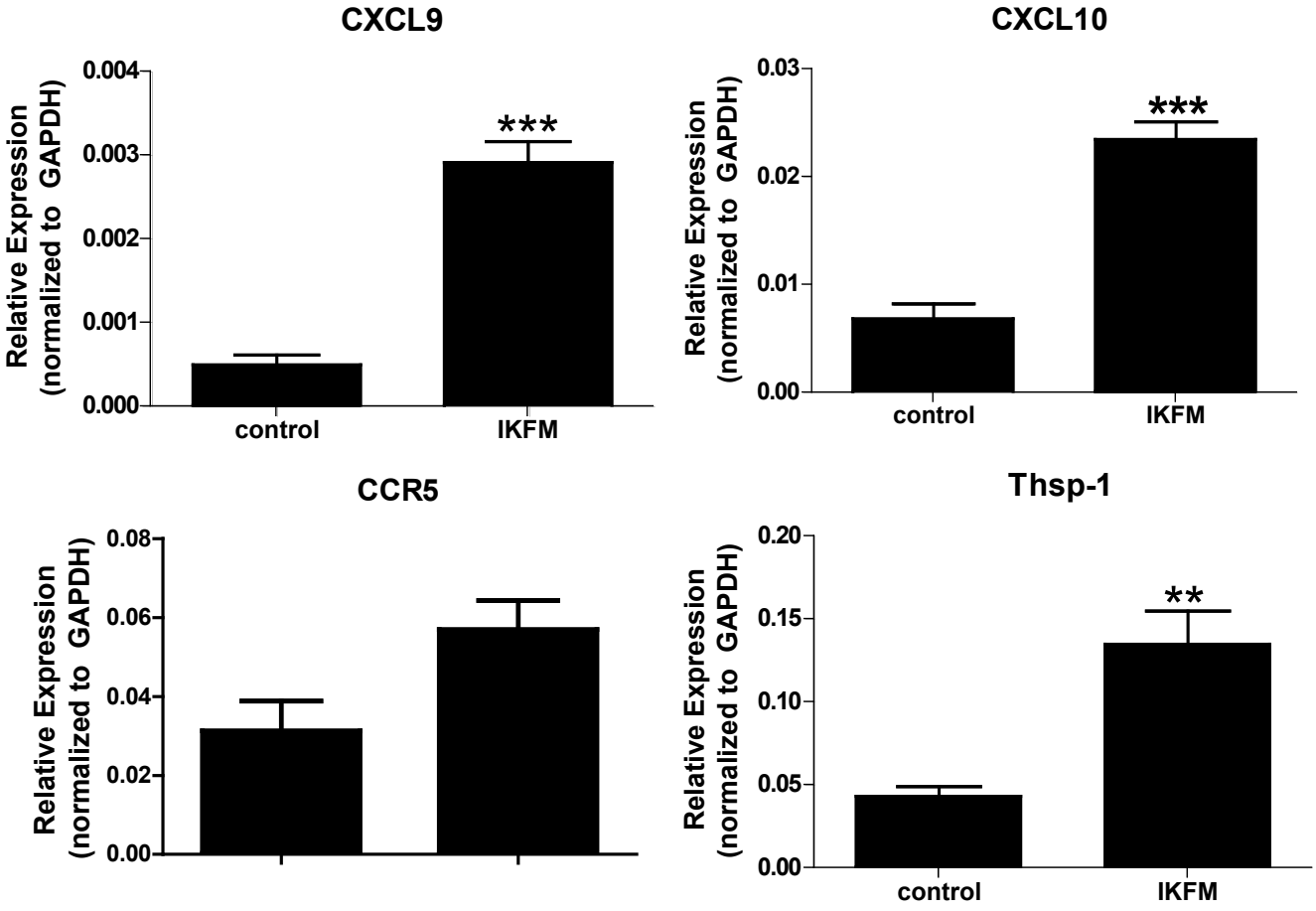

Generate IKFM PyVT mice and determine effects of increased NF-κB activity in macrophages on lung metastasis from a primary mammary tumor. The tail vein metastasis model used above did not display the pro-tumor effect that we were predicting would occur in the presence of TAMs with increased NF-κB activity. To address this question in a model with more established tumors we mated homozygous c-fms rtTA transgenics with PyVT mice to generate double transgenic breeder males. These were mated with IKK females to generate experimental animals including IKFM and PyVT.

PyVT mice rapidly produce multifocal mammary adenocarcinomas together with secondary metastatic tumors in the lung by 12 weeks (9,10). Female triple transgenics and control littermates were palpated twice weekly from 7 weeks until detection of primary palpable mammary tumor. Our original intention was to treat mice with dox (plus littermate controls) from this point until lung harvest 6 weeks later. This strategy was adopted to more closely mimic the full biological process of metastasis from a primary tumor to the lungs. However, treatment of a triple transgenic female with dox resulted in a very detrimental phenotype. The first IKFP triple transgenic after only 28 days of dox treatment appeared lethargic. It had a hunched, feeble appearance, with legs tucked beneath it. The feet and ears were pale yellow in color. The area around the eyes was red and inflamed. Although the mouse had been alone in its cage, the tail had scab marks and was swollen at its base, with unexplained bulges throughout. Upon dissection, mammary tumor burden was average compared to age matched polyoma mice. Gross anatomy of the lungs, kidneys and digestive tract appeared normal. However, the spleen was very enlarged and the liver showed some white, marbled

patches. Therefore, at 28 days of treatment we decided to sacrifice the animal for humane reasons and to discontinue this approach. We do not fully understand why in this model induction of increased NF-κB activity in the macrophages makes the animals so sick when we have been able to treat double transgenic mice in the tail vein studies for an equivalent time without observing these effects. We believe that there is some co-operation between the inflammatory state induced by the tumor load in this model and that of the modified macrophages that may establish a pro-inflammatory feed back loop which has these strong pathogenic effects.

As prolonged treatment of IKFP triple transgenics appears to have major detrimental effects we adopted a new approach. At 7 weeks of age, we began palpation of IKFP mice and controls which contained the polyoma transgene but lacked one or both of the other components, twice per week. After detecting the first primary tumor via palpation, we waited 20 days and then began dox treatment (0.5 g/L) for an additional 10 days followed by sacrifice (sac was at 30 days post palpable tumor). This strategy helped reduce the morbidity within the IKFP group, as triple transgenics treated with dox for only 10 days showed some signs of inflammation, but none were exhibiting advanced symptoms that would require early sacrifice (as in the 30 day treated group). A total of 6 IKFP triple transgenics and 14 littermate controls were collected according to this new protocol. At sacrifice, we measured the total gland weight, determined the volume of the largest primary tumor, and inflated lungs for metastasis counts. Total gland weight was not significantly different among the groups (p=0.8522). The number of lung metastasis were also not significantly different. The largest primary tumor volume trended towards on average, a larger tumor being present in the control mice, but this would need further investigation. The generation of triple transgenics is time and effort intensive and the spontaneous tumors that arise in the polyoma mice are somewhat variable, therefore, we believe that future studies would be more effectively performed using a primary orthotopic tumor model.

Task 2. Determine effects of decreased NF-κB activity in macrophages on lung metastasis:

Determine effects of decreased NF-κB activity in macrophages on lung tumor development using a tail vein metastasis model.

To determine whether the opposite effect was observed when NF-κB is inhibited in the macrophages in our tail vein injection model, PY1 cells were introduced via the tail vein into immunocompetent

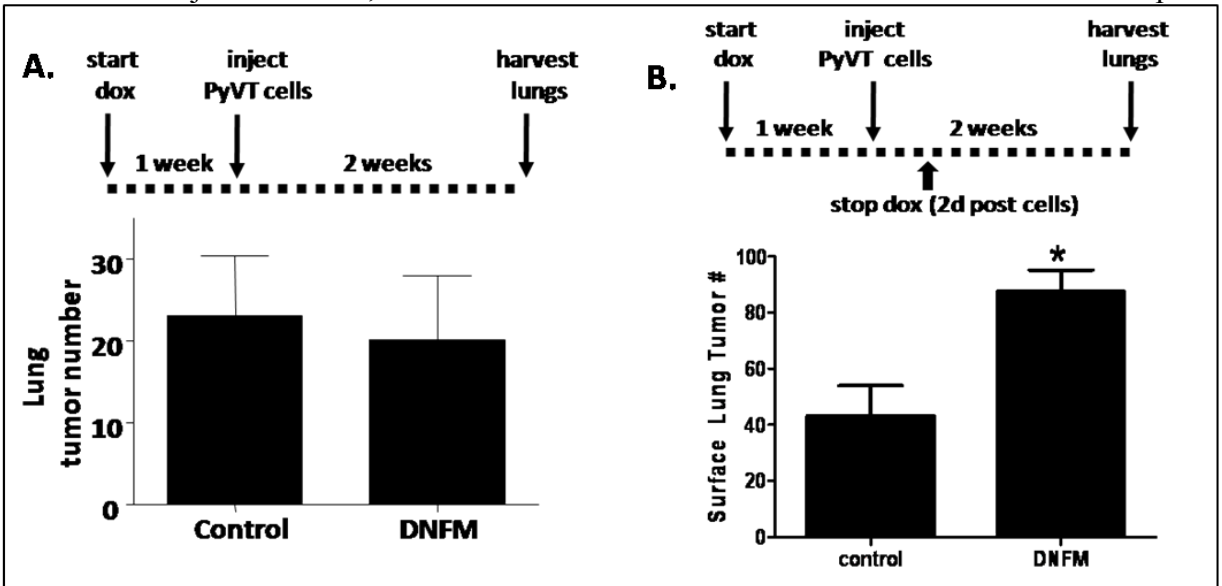

Figure 6. **DNFM mice and controls were treated with dox 1 week prior to cell injection and treatment was continued until the time of sacrifice. Surface lung tumor counts (A) revealed no significant difference in control vs. DNFM (n= 6 controls, n=8 DNFM, p=0.7977). In a separate experiment, DNFM mice and controls were treated with dox 1 week prior to cell injection. Dox treatment was discontinued 2 days after cell injection, and mice were harvested at 2 weeks post cells. Surface lung tumor counts (B) show tumor burden significantly increased in DNFM vs. control (n= 6 control, n=9 DNFM, p = 0.0039).**

DNFM and control mice. Experimental subsets included DNFM and control littermates with dox provided at 2mg/ml in 5% sucrose drinking water *ad lib* for this and all following dox induction experiments. Dox treatment started 1 week prior to PY1 cell injection and continued until harvest at 2 weeks post cell injection. At the end point the number of surface lung metastases was quantified (Figure 6A and Connelly *et al* 2011). We detected no significant difference in the numbers of lung metastases in mice in which NF-κB activity was inhibited in the macrophages throughout the study. Given the data obtained from the IKFM mice that suggested that an anti-tumor effect was observed early in the metastatic process and that no effect was seen for modulation of NF-κB from 2 days after introduction of the cells together with our suspicion that this model was not optimal for investigation of later stage TAM-related effects, we decided to concentrate on the time point that was producing the most interesting data ie. dox treatment for 1 week prior to cell introduction until 2 days post cell introduction.

*Determine effects of decreased NF-κB activity in macrophages at **early stages** of metastasis on lung tumors using a tail vein metastasis model.*

The data obtained from studies using the IKFM mice suggests a strong anti-tumor influence of increased NF-κB activity in macrophages at very early stages of the metastatic process. We performed similar studies using the DNFM mice to determine whether these resulted in the opposite effect. PY1, 2 or 3 cells were introduced via the tail vein with the same experimental strategy as above. Dox treatment started 1 week prior to cell injection and continued until 2 days post cell injection. Lungs were harvested at 2 weeks (PY1 and PY3) or 5 weeks (PY2) post cell injection (Figure 6B and Connelly *et al* 2011). The subset of mice that were injected with PY1 demonstrated a significant pro-tumor impact of inhibition of NF-κB activity in the early stage of metastasis. PY3 cells exhibited the same trend but the numbers in the subset of mice that we used in this study did not reach significance (p= 0.1564). We believe that these results represent an indication that inhibition of NF-κB in macrophages during early stages of metastasis can have a pro-tumor impact. Given the limited time and resources we decide to focus on determining the changes in the microenvironment and the mechanisms that led to the significant impact in the IKFM model.

*Determine effects of decreased NF-κB activity in macrophages at **later stages** of metastasis on lung tumors using a tail vein metastasis model.*

We originally proposed to investigate the effects on decreasing NF-κB activity in macrophages during the later stages of metastasis using the tail vein model. However, the data that we obtained from our other studies strongly suggests that we would not observe an impact, potentially due to limitations of the model. Therefore, we decided to focus on other questions and time points.

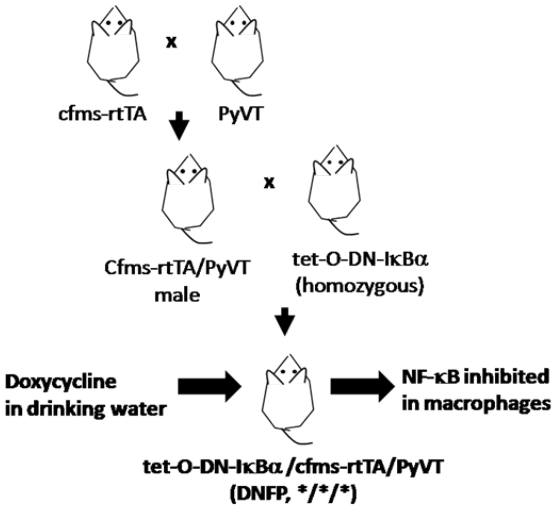

Figure 7. **Breeding strategy for generation of a */*/* DNFP triple transgenic. (*/-/* mice used as controls do not contain the cfms rtTA).**

Generate DNFM PyVT mice and determine effects of increased NF-κB activity in macrophages on lung metastasis from a primary mammary tumor. Our original hypothesis suggested that inhibition of NF-κB activity in macrophages would inhibit mammary to lung metastasis. While the data from our tail vein studies did not support this idea, we were concerned that the tail vein model did not allow investigation of effects in the presence of established tumor. Therefore we mated homozygous c-fms

rtTA transgenics with PyVT mice to generate double transgenic breeder males. These were mated with homozygous DN females to generate experimental animals including DNFM and PyVT (Figure 7). Female triple transgenics and littermate controls were palpated twice weekly from 7 weeks until detection of primary palpable mammary tumor. Mice were treated with dox from this point until mammary and lung harvest 30 days later (Figure 8). To attempt to minimize variability in our studies we use littermates as experimental animals and controls. Generation of the triple transgenic mice can be variable within age-matched litters. The first time that we ran through this experimental protocol we believed that we had included 7 triple transgenics and 5 control littermates. However, upon confirming the genotyping at the end of the study we discovered that one mouse had been mis-genotyped and we actually had 8 triple transgenics and 4 control littermates. The data from this set was significant and suggested that inhibition of NF-κB activity in the macrophages in this model resulted in decreased primary mammary tumor load and decreased numbers of lung metastases. This was very intriguing as it suggested that inhibition of NF-κB could be pro-tumor in our tail vein metastasis model but anti-tumor in the model in which a primary tumor is developing. The observed effect on primary tumor would agree with our original hypothesis and with the recently published data from other groups that suggests that in some models NF-κB activity in macrophages has pro-tumor effects. We completed TUNEL staining on mammary sections harvested at the endpoint to quantify levels of apoptosis both over the tissue as a whole and by defining hyperplasia, adenoma and carcinoma as different stages of mammary tumor progression. We did not detect any significant changes in apoptosis between triple transgenics and controls in the tissue as a whole or in defined stages (data not shown).

We were concerned about the relatively low number of mice in the control group so we decided to generate additional mice to increase the numbers in each group (Second Set – Figure 8).

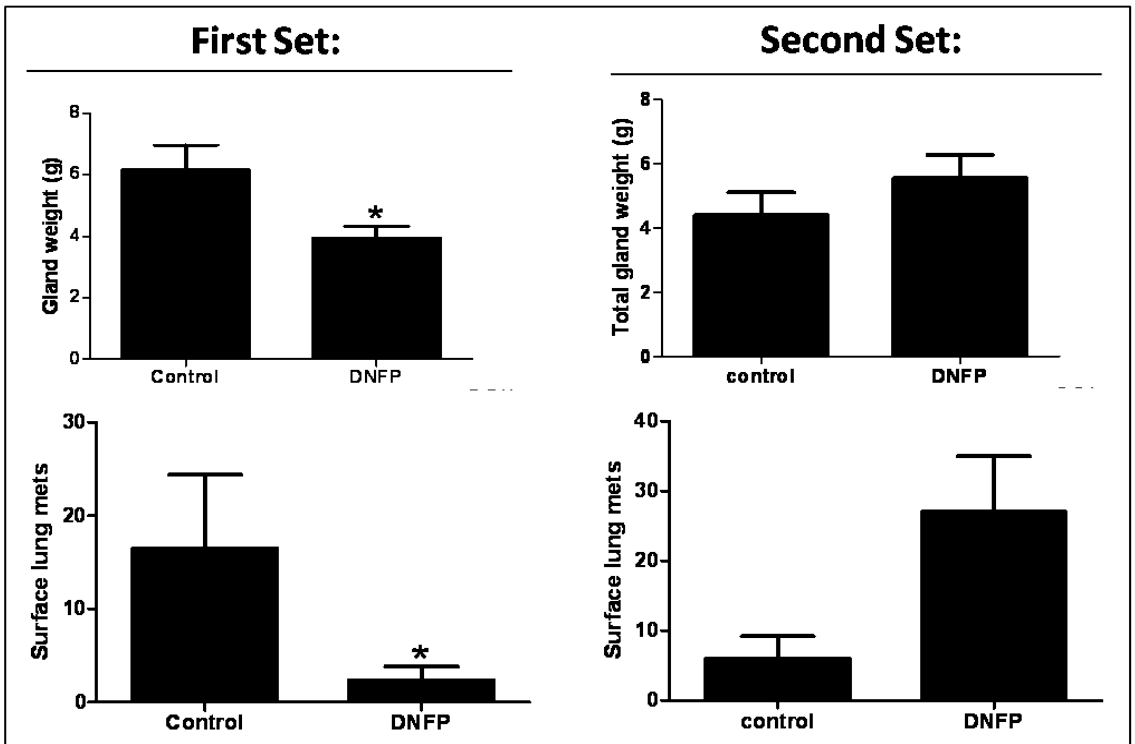

Figure 8. **DNFP triple transgenics and litttermate controls (did not contain cfms-rtta transgene) were palpated until the first primary tumor was found. At that time, mice were put on dox treatment for 30 days, then harvested and mammary glands weighed for a total gland weight. Lungs were inflated with Bouin's fixative and surface lung tumors were counted under a dissecting microscope. Two sets were collected. The first set (n=4 control, n=8 DNFP) showed significant decrease in tumor burden in the DNFP mice vs control (p = 0.0177) as well as significantly reduced lung tumor numbers in DNFP (p=0.0325). However, the second set (n=3 control, n=4 DNFP) did not show a significant difference in either end-point (p=0.311 and p=0.0868 respectively).**

The results from this set were not significant. Combining the data from all animals resulted in non-significant results for the group as a whole. We rechecked all the mice from both groups for expression of the DN transgene by RT-PCR and all triple transgenics are expressing the transgene. We must conclude from the available data that there is no significant effect of inhibition of NF-κB as tested in this model. Having three transgenic component parts within the model each with some inherent variability may be obscuring important findings, therefore, we believe that a different strategy will be necessary to address this question.

We decided that the question may be better addressed using an orthotopic tumor model. DNFM females and controls (n=5 controls and n=5 DNFM) were injected with $1x10^6$ L129 polyoma tumor cells at day 0 of the study. 2 weeks post injection, tumors were determined to be of measureable size (> 50 cm3). Dox treatment (2 g/L) began and primary tumor measurements were taken every other day for the remainder of the study. All mice were harvested after 2 weeks of dox treatment (day 14 post palpable tumor), as some tumors reached volumes over 1000 cm^3. The tumor growth curve and tumor weights at endpoint were similar among the two groups (no significant difference). One DNFM and one control mouse showed signs of metastasis to lung, although both lungs showed similar numbers of "possible" metastasis (5 and 2 respectively), and other lungs collected for both groups showed no signs of metastasis. The cell line that we used for this pilot study is one of our most aggressive polyoma-derived lines with rapid progression. We may need to use a slower growing line to determine impacts on primary tumor growth. Conversely, in order for metastases to develop in the majority of test animals it may be necessary to amend the protocol for surgical removal of the orthotopic primary once it reaches the largest size approved by the local IACUC committee (likely to be 1.5cm) to allow experimental animals to be maintained for a longer period of time and for metastases to develop.

KEY RESEARCH ACCOMPLISHMENTS

1) We have investigated the effects of increased NF-κB activity in macrophages in a tail vein metastasis model and obtained unexpected data that suggest that this results in a strong anti-tumor effect but only during early stages of metastasis.
2) Our data using a tail vein metastasis model suggests that decreased NF-κB activity in macrophages during early stages of metastasis can have pro-tumor effects.
3) We have started to elucidate some of the mechanisms leading to the observed phenotypes.
4) Our studies combining our inducible macrophage model with the polyoma model of mammary tumorigenesis are inconclusive due in part to technical issues. Our data suggests that prolonged induction of NF-κB in macrophages concurrently with a relatively large primary tumor load may generate a hyper-inflammatory feedback loop. While one group of mice suggested an impact of inhibition of NF-κB on primary tumor development, a second set of mice failed to confirm this observation.

REPORTABLE OUTCOMES

Manuscripts

Connelly, L., Barham, W., Onishko, H.M., Chen, L., Sherrill, T.P., Zabuawala, T., Ostrowski, M.C., Blackwell, T.S., Yull, F.E. (2011) NF-kappaB activation within macrophages leads to an anti-tumor phenotype in a mammary tumor lung metastasis model. Breast Cancer Research In Press.

Blackwell, T.S., Hipps, A.N., Yamamoto, Y., Han, W., Barham, W.J., Ostrowski, M.C., Yull, F.E., Prince, L.S. (2011) NF-κB signaling in fetal lung macrophages. J. Immunology 187:2740-2747.

Presentations
Research Assistant 1 Whitney Barham gave invited presentation at the annual Host-Tumor Interactions Program and Department of Cancer Biology 9th annual joint retreat Nov 2009 titled "Modulation of NF-κB in Macrophages can produce both pro- and anti-tumor effects during mammary tumor progression"

Research Assistant 2 Whitney Barham gave invited presentation at the annual Host-Tumor Interactions Program and Department of Cancer Biology 10th annual joint retreat titled "Cell specificity and timing of targeted NF-kappaB modulation determines potential for therapeutic outcome during mammary tumorigenesis".

Research Assistant 2 Whitney Barham gave invited presentation at the annual AACR meeting titled "Inducible modulation of NF-κB in macrophages reveals that timing of intervention may be critical to therapeutic outcome during mammary tumorigenesis".

Abstracts
Poster presentation at the Cancer and Inflammation Keystone Symposium Feb 2010
Poster presentation at the AACR 101st Annual Meeting April 2010
Poster presentation at the Vanderbilt Ingram Cancer Center retreat May 2010
Poster presentation at the DOD Era of Hope August 2011

Animal models
We have established the feasibility of using our novel inducible macrophage targeted transgenics to investigate the effects of modulating NF-κB activity in macrophages on mammary tumorigenesis. In addition, these novel models have been used in collaborative studies demonstrating a contribution of NF-κB activity to a pathogenic role of activated macrophages in bronchopulmonary dysplasia, a dangerous complication of preterm birth caused by an arrest in airway morphogenesis (Blackwell *et al* 2011 – appended).

Funding applications
BC101825 DOD Breast Cancer Program IDEA application titled "Timing of NF-kappaB modulation during tumor progression is critical for therapeutic outcome". Not funded.

BC102696P1 DOD Breast Cancer Program IDEA: Collaborative Option application titled "Development and Testing of Therapeutic Potential of Nanobiotechnology-Targeted siRNA Designed to Inhibit NF-κB Classical & Alternative Signaling in Macrophages". Holder of this grant is Partnering PI on funded proposal.

NIH RO1 entitled "Macrophage-targeted modulation of NF-kappaB to inhibit mammary cancer metastasis" submitted June 2011.

Susan G. Komen Foundation Investigator Initiated grant proposal pre-application submitted entitled "Exploiting macrophages to block breast cancer progression and metastasis".

LC110242 DOD Lung cancer program pre-application submitted entitled "Harnessing the power of the immune system for eradication of lung cancer".

Personnel receiving pay from research effort
Fiona Yull - PI
Lianyi Chen – RA1
Whitney Barham – RA2
Halina Onishko – RA3

CONCLUSIONS

When we initiated these studies our hypothesis was that NF-κB activity in macrophages determines metastatic potential and thus represents a target for inhibition of metastatic breast cancer. We were expecting that increasing NF-κB in macrophages would skew them towards a pro-tumor tumor-associated macrophage (TAM) phenotype. We were also predicting that these macrophages would induce a chronic inflammatory environment that would support tumor metastasis by increasing angiogenic and matrix remodeling signals. We proposed to address two questions. 1) Does activation of NF-κB in macrophages contribute to mammary metastasis? 2) Can inhibition of NF-κB in macrophages inhibit mammary to lung metastasis? Our data suggests that the role of NF-κB in macrophages is more complex than we believed. Contrary to our expectations, activation of NF-κB in macrophages at early stages of metastasis appears to exhibit powerful anti-tumor effects. Futhermore, indications are that inhibition of NF-κB in macrophages at this early stage can have pro-tumor impact, and there remains in place evidence that NF-κB in macrophages at later stages may also have pro-tumor effects. It appears that NF-κB activity in macrophages does determine metastatic potential and may represent a target for inhibition of metastatic breast cancer but that the timing of such an intervention during the progression of the tumor may be critical to therapeutic outcome. There are efforts being made to develop inhibitors of NF-κB as potential therapeutics for the treatment of breast cancer. Our data may suggest that inhibition of NF-κB in a patient with circulating metastatic tumor cells may be counter-productive. We are pleased to report the acceptance of a manuscript leading directly from these studies in the journal "Breast Cancer Research" (manuscript appended).

REFERENCES

1) Cheng, D. S., W. Han, S. M. Chen, T. P. Sherrill, M. Chont, G. Y. Park, J. R. Sheller, V. V. Polosukhin, J. W. Christman, F. E. Yull, and T. S. Blackwell. (2007) Airway epithelium controls lung inflammation and injury through the NF-kappa B pathway. J Immunol 178:6504-6513 (co-senior authorship).

2) Yan C, Lian X, Li Y, Dai Y, White A, Qin Y, Li H, Hume DA, Du H. (2006) Macrophage-specific expression of human lysosomal acid lipase corrects inflammation and pathogenic phenotypes in lal-/- mice.
Am J Pathol. 169:916-26.

3) Stathopoulos, GT, Sherrill, TP, Cheng, D-s, Scoggins, RM, Han, W, Polosukhin, VV, Connelly, L, Yull, FE, Fingleton, B, Blackwell, TS (2007) Epithelial nuclear factor-kappaB activation promotes urethane-induced lung carcinogenesis. Proc Natl Acad Sci 104:18514-9.

4) Fong, C.H., Bebien, M., Didierlaurent, A., Nebauer, R., Hussell, T., Broide, D., Karin, M., Lawrence, T. (2008) An antiinflammatory role for IKKbeta through the inhibition of "classical" macrophage activation. J Exp Med 205:1269-76.

5) Greten, F.R., Eckmann, L., Greten, T.F., Park, J.M., Li, Z.W., Egan, L.J., Kagnoff, M.F., Karin, M. (2004) IKKbeta links inflammation and tumorigenesis in a mouse model of colitis-associated cancer. Cell 118:285-96.

6) Hagemann, T., Lawrence, T., McNeish, I., Charles, K.A., Kulbe, H., Thompson, R.G., Robinson, S.C., Balkwill, F.R. (2008) "Re-educating" tumor-associated macrophages by targeting NF-kappaB. J Exp Med 205:1261-8.

7) Mantovani, A., Allavena, P., Sica, A., Balkwill, F. (2008) Cancer-related inflammation. Nature 454:436-44.

8) Timmer, A.M., Nizet, V. (2008) IKKbeta/NF-kappaB and the miscreant macrophage. J Exp Med 205:1255-9.

9) Guy, C.T., Cardiff, R.D., Muller, W.J. (1992) Induction of mammary tumors by expression of polyomavirus middle T oncogene: a transgenic mouse model for metastatic disease. Mol Cell Biol. 12:954-61.
10) Lin, E.Y., Jones, J.G., Li, P., Zhu, L., Whitney, K.D., Muller, W.J., Pollard, J.W. (2003) Progression to malignancy in the polyoma middle T oncoprotein mouse breast cancer model provides a reliable model for human diseases. Am J Pathol. 163:2113-26.

APPENDICES

Abstract for Inflammation and Cancer Keystone Symposium

Activation of NF-κB in macrophages inhibits mammary metastasis to lung in a tail vein model

L Connelly, W Barham, H Onishko, A Newsome, T Sherrill, T Zabuawala, M Ostrowski, T Blackwell, F Yull.

Macrophages can exhibit both pro and anti-tumor functions and NF-κB signaling can regulate genes that mediate these effects. However, the role of NF-κB signaling in directly influencing macrophage contribution to mammary tumorigenesis is largely unknown. We have generated a doxycycline inducible transgenic model that enables modulation of NF-κB signaling within macrophages through expression of a constitutively active form of IKK2, the upstream kinase in the classical NF-κB cascade. In this model, the c-fms promoter drives macrophage specific expression of the reverse tetracycline transactivator (rtTA). Administration of doxycycline in drinking water allows the rtTA protein to bind to the Tet operon, driving IKK2 transgene expression and constitutive NF-κB activity within macrophages.
We are using this model in tail vein metastasis studies with mammary tumor cell lines derived from the Polyoma model of mammary tumorigenesis. Our data suggest that increased NF-κB activity within macrophages can enhance host defense and have anti-tumor effects at least during early stages of tumorigenesis. These effects may be mediated by modulation of expression of genes that define M1 versus M2 macrophage types. Although recent data suggests that NF-κB activity within tumor associated macrophages can be pro-tumor, our model argues that at earlier stages of tumor development NF-κB activity within macrophages may have opposite effects.

Abstract for AACR 101st Annual Meeting

Macrophage specific regulation reveals both pro- and anti-tumor effects of NF-kappaB during mammary tumor progression

L Connelly, W Barham, H Onishko, T Zabuawala, M Ostrowski, T Blackwell and F Yull

An increased level of macrophages in human tumors is associated with a poorer prognosis. The transcription factor Nuclear Factor-kappaB (NF-kappaB) is an important regulator of gene expression within macrophages. Recent studies point to a pro-tumorigenic role for NF-kappaB activity in macrophages; however NF-kappaB also regulates expression of genes such as inducible nitric oxide synthase which are associated with anti-tumor effects. We believe that NF-kappaB activity in macrophages can have both anti- and pro-tumor effects depending on tumor stage.
We have developed novel murine models to determine the effects of modulation of NF-kappaB activity specifically within macrophages during primary mammary tumor growth and metastasis. We have used the cfms promoter to specifically express the reverse tetracycline transactivator (rtTA) protein in macrophages. The rtTA can drive tet operon regulated gene expression in the presence of doxycyline (dox). We have used this with a dominant negative IkappaB alpha (DN-IkappaBalpha) to inhibit NF-kappaB signaling in the Polyoma mouse mammary tumor model, this model is termed DNFP. We have also used the cfms-rtTA in combination with a constitutively active IKK2 transgene to activate NF-kappaB signaling, this model is termed IKFM.
When NF-kappaB is inhibited in macrophages during primary tumor growth in our DNFP model there is a reduction in primary tumor growth accompanied by a reduced level of lung metastasis. This data suggests that NF-kappaB in macrophages is acting in a pro-tumor manner, in agreement with recently published data. In contrast, we have found that activation of NF-kappaB in

macrophages by treating IKFM mice with doxycycline for 1 week before and during two weeks following tail vein injection of polyoma mammary tumor cells leads to a significant reduction in surface lung tumor formation. In additional studies, IKFM mice were pretreated with dox for 1 week but treatment was stopped two days after tumor injection. A similar reduction in tumor number was observed, suggesting an inhibition of cell seeding. Real time PCR analysis of lungs from mice with activation of NF-kappaB in macrophages suggests an anti-tumor "M1" macrophage phenotype.
In summary, our data indicates that NF-kappaB activity in macrophages can have both anti- and pro-tumor effects dependent on tumor stage. This data would suggest that cell specificity and timing of treatment are important considerations with regards to the use of NF-kappaB inhibitors in cancer treatment

Abstract for Host-Tumor Interactions Program and Cancer Biology 10th annual joint retreat Nov 2010

Cell specificity and timing of targeted NF-kappaB modulation determines potential for therapeutic outcome during mammary tumorigenesis

Whitney Barham, Halina Onishko, Lianyi Chen, Linda Connelly, Fiona Yull

Elevated levels of NF-kappaB signaling are associated with multiple cancers therefore it is not surprising that inhibitors of NF-kappaB are being investigated as potential therapeutics. While extensive efforts are being made to identify inhibitors there is less focus on investigating the effects of inhibition in specific cell types and during defined stages of tumor progression. We have developed murine transgenic models that enable us to induce expression of an activator or inhibitor in specific cell types, mammary epithelium or macrophages, by adding doxycycline to the drinking water of mice. We have combined these with the Polyoma model of mammary cancer. Our data suggest that inhibition of NF-kappaB in mammary epithelium limits tumor progression. Additionally, systemic treatment with a pharmacologic inhibitor thymoquinone limits growth of orthotopic polyoma mammary tumors. However, we have also obtained data that identifies a stage during progression in which activation of NF-kappaB in macrophages limits metastasis. Activation of NF-kappaB alters immune cell populations and results in rapid killing of tumor cells during the seeding phase in a tail vein metastasis model. This suggests that inhibition of NF-kappaB during metastasis may have an undesirable impact on tumor progression. Our studies highlight the importance of continued investigation into aspects of cell specificity and timing that may change the potential outcome of a clinical trial using NF-kappaB inhibitors.

Abstract for AACR 102st Annual Meeting April 2011

Inducible modulation of NF-kappaB in macrophages reveals that timing of intervention may be critical to therapeutic outcome during mammary tumorigenesis

Whitney Barham, Linda Connelly, Halina Onishko, Lianyi Chen, Taylor Sherrill, Tahera Zabuawala, Mike Ostrowski, Timothy S. Blackwell, and Fiona E. Yull

Elevated levels of NF-kappaB signaling are associated with multiple cancers. Therefore, it is not surprising that inhibitors of NF-kappaB are being investigated as potential therapeutics. While extensive efforts are being made to identify inhibitors there is less focus on investigating the effects of inhibition in specific cell types and during defined stages of tumor progression. We have developed murine transgenic models that enable us to induce expression of an activator or inhibitor of NF-kappaB in macrophages, by adding doxycycline to the drinking water of mice. We have combined these with the Polyoma model of mammary cancer to investigate the effects of modulation of NF-kappaB signaling specifically within macrophages. Given several recent publications we were predicting that activation of NF-kappaB would have pro-tumor effects. However, using a tail vein injection model, our data identifies a stage during progression in which activation of NF-kappaB in macrophages significantly limits metastasis. Activation of NF-kappaB alters immune cell populations and results in rapid killing of tumor cells during the seeding phase. In this model inhibition of NF-kappaB in macrophages during this critical stage of metastasis is pro-tumor. This suggests that while inhibition of NF-kappaB at later stages of tumor progression may have

therapeutic benefit, inhibition during the seeding phase my lead to the opposite effect. Our studies highlight the importance of continued investigation into aspects of cell specificity and timing that may change the potential outcome of a clinical trial using NF-kappaB inhibitors.

Abstract for DOD Era of Hope Meeting August 2011

NF-kappaB activation within macrophages leads to an anti-tumor phenotype in a lung metastasis model

Linda Connelly, Whitney Barham, Halina M. Onishko, Lianyi Chen, Taylor Sherrill, Tahera Zabuawala, Michael C. Ostrowski, Timothy S. Blackwell Fiona E. Yull

Inflammation, cancer and immune responses are linked. Macrophages contribute to these processes and are regulated by NF-kappaB transcription factors. However, our knowledge of the contribution of NF-kappaB specifically within macrophages is extremely limited. To investigate NF-kappaB signaling within macrophages during metastasis, we developed novel inducible transgenic models. By targeting expression of the reverse tetracycline transactivator (rtTA) to macrophages using the cfms promoter in combination with inducible transgenics that express either an activator (cIKK2) or an inhibitor (IkappaBalpha-DN), doxycyline treatment led to activation or inhibition of NF-kappaB within macrophages. We used a tail vein metastasis model with mammary tumor cell lines derived from MMTV-Polyoma Middle T-Antigen-derived tumors to investigate the effects of modulating NF-kappaB in macrophages during different temporal windows of the metastatic process. We found that activation of NF-kappaB in macrophages before tumor cells were introduced leads to a reduction in lung metastases. The mechanism involved expression of inflammatory cytokines and reactive oxygen species, leading to apoptosis of tumor cells and preventing seeding in the lung. Our results have identified a brief, defined window in which activation of NF-kappaB has significant anti-metastatic effects and inhibition of NF-kappaB results in a worse outcome.

NF-kappaB activation within macrophages leads to an anti-tumor phenotype in a mammary tumor lung metastasis model

Linda Connelly[1,2+], Whitney Barham[1+], Halina M Onishko[1], Lianyi Chen[1], Taylor Sherrill[3], Tahera Zabuawala[4], Michael C Ostrowski[4], Timothy S Blackwell[1,3,5] and Fiona E Yull[1,*]

[1] Department of Cancer Biology, Vanderbilt University, 771 Preston Research Building, 2220 Pierce Avenue, Nashville, TN 37232, USA

[2] Department of Pharmaceutical Sciences, UH Hilo College of Pharmacy, University of Hawaii at Hilo, 200 W. Kawili Street, Hilo, HI 96720, USA

[3] Division of Allergy, Pulmonary and Critical Care Medicine, Department of Medicine, Vanderbilt University, T-1217 Medical Center North, Nashville, TN 37232, USA

[4] Department of Molecular and Cellular Biochemistry, The Comprehensive Cancer Center, Ohio State University, 810 Biomedical Research Tower, 460 W. 12th Avenue, Columbus, OH 43210, USA

[5] Department of Veterans Affairs, T-1217 Medical Center North, Nashville, TN 37232, USA

[+] contributed equally

* correspondence: fiona.yull@vanderbilt.edu

Abstract

Introduction

Metastasis from primary tumor to the lungs is a major cause of the mortality associated with breast cancer. Both immune and inflammatory responses impact whether circulating mammary tumor cells successfully colonize the lungs leading to established metastases. Nuclear factor - kappaB (NF-κB) transcription factors regulate both immune and inflammatory responses mediated in part by the activities of macrophages. Therefore, NF-κB activity specifically within macrophages may be a critical determinant of whether circulating tumor cells successfully colonize the lungs.

Methods

To investigate NF-κB signaling within macrophages during metastasis, we developed novel inducible transgenic models which target expression of the reverse tetracycline transactivator (rtTA) to macrophages using the *cfms* promoter in combination with inducible transgenics that express either an activator (cIKK2) or an inhibitor (IκBα-DN). Doxycyline treatment led to activation or inhibition of NF-κB within macrophages. We used a tail vein metastasis model with mammary tumor cell lines established from MMTV-Polyoma Middle T-Antigen-derived tumors to investigate the effects of modulating NF-κB in macrophages during different temporal windows of the metastatic process.

Results

We found that activation of NF-κB in macrophages during seeding leads to a reduction in lung metastases. The mechanism involved expression of inflammatory cytokines and reactive oxygen species, leading to apoptosis of tumor cells and preventing seeding in the lung. Activation of NF-

κB within macrophages after the seeding phase has no significant impact on establishment of metastases.

Conclusions

Our results have identified a brief, defined window in which activation of NF-κB has significant anti-metastatic effects and inhibition of NF-κB results in a worse outcome.

Introduction

The microenvironment that exists during chronic inflammation can contribute to cancer progression [1, 2]. Therefore, anti-inflammatory strategies are being investigated as potential cancer therapies. However, such approaches may have undesired effects on host immune responses. Potentially, these negative effects could be limited by targeting interventions to specific cell types, but little is known about the contribution of individual inflammatory cell types to the progression of cancer.

The transcription factor Nuclear Factor kappa B (NF-κB) regulates inflammatory status and plays key roles in immune responses. NF-κB is a dimer formed from a multi-subunit family consisting of p65 (Rel A), Rel B, c-Rel, p105/p50 (NF-κB1), and p100/p52 (NF-κB2) [3, 4]. In the classical NF-κB signaling pathway the p50/p65 subunits are held in the cytosol by the inhibitory IκBα [5, 6]. During activation the IκB kinase (IKK) 2 phosphorylates IκBα leading to ubiquitination and degradation. P50/p65 then translocates into the nucleus, binds to consensus DNA sequences activating expression of target genes [3, 6, 7]. We and others have modulated this signaling using a constitutive form of IKK2 to activate or a mutant form of IκBα to inhibit NF-κB activity [8-10].

Macrophages are key mediators of the interaction between inflammation, immunity and cancer. The role of macrophages in cancer has received attention due to the discovery of their tumor-promoting effects [11-13]. Efforts have been made to classify macrophages according to phenotype. The M1 macrophage phenotype is associated with production of reactive oxygen species (ROS), presentation of antigens, release of inflammatory cytokines and cytotoxic effects on pathogens and tumor cells. In contrast, the M2 macrophage phenotype has a reduced ability to present antigens and produce ROS, expresses scavenger receptors, promotes angiogenesis and

wound healing and is associated with tumor promoting effects [14, 15]. However, tumor-associated macrophages (TAMs) can express genes associated with both the M1 and M2 phenotypes highlighting the need for further investigation into macrophage phenotype during tumorigenesis [16].

Recent studies have investigated the role of NF-κB in macrophages during tumorigenesis. A LysM-Cre/floxed IKK2 transgenic, resulting in deletion of IKK2 in cells of the myeloid lineage (macrophages and granulocytes), led to a reduction in colon tumor incidence and size in a colitis-associated cancer model [17]. An IκB-super repressor targeted to Kupffer cells (liver macrophages) led to a similar reduction in tumor incidence in a murine model of hepatocellular carcinoma [18]. It has been reported that TAMs can induce invasive behavior of ovarian tumor cells via NF-κB [19, 20]. In established orthotopic ovarian tumors, the introduction of macrophages with inhibited IKK2 led to a reduction in tumor burden. These effects were associated with a switch from M2 to M1 phenotype upon NF-κB inhibition [21]. These studies suggest a tumor-promoting effect of NF-κB in myeloid cells, including macrophages.

Despite these data pointing to a pro-tumor role for NF-κB in macrophages, genes regulated by NF-κB could also lead to an anti-tumor phenotype, suggesting that effects may be more complex. We have generated transgenic mouse models to modulate NF-κB in specific tissues by introducing doxycycline (dox) in drinking water [8, 10]. To investigate NF-κB signaling within macrophages during metastasis we used a bi-transgenic system in which the Colony Stimulating Factor 1 Receptor promoter (cfms) drives the monocyte/macrophage-specific expression of the reverse tetracycline transactivator (rtTA). To activate NF-κB, the cfms-rtTA mouse was crossed with a second transgenic in which constitutively active IKK2 (cIKK2) was controlled by the tet operon (termed IKFM). To inhibit NF-κB, cfms-rtTA is

crossed with a transgenic line in which dominant negative IκBα is controlled by the tet operon (termed DNFM). We used these models in a mouse mammary tumor cell tail vein-injection metastasis model that is extensively used as a methodology to investigate the later stages of the metastatic process from the point at which circulating tumor cells are present. We find that activation of NF-κB in macrophages during a short window around the time of cell injection leads to a reduction in lung metastasis of mammary tumor cells. The mechanism involves induction of an anti-tumor M1 phenotype that rapidly clears tumor cells. Two days after injection of tumor cells this window of opportunity closes and from this point activation of NF-κB no longer exhibits anti-tumor effects.

Materials and methods

Tumor cells

PyVT R221A and PYG 129 polyoma tumor cells were isolated from PyVT mammary gland tumors and cultured as previously described [9] [22].

Mouse strains

All animal experiments were approved by the Vanderbilt University Institutional Animal Care and Use Committee. All mice were on an FVB strain background, except the TG/CRE/FMR mice which were mixed background (C57BL6 and FVB).

To generate the cfms-rtTA transgenic, the 7.2kb mouse *cfms* promoter region was used to drive the expression of *rtTA-M2* [23]. The *cfms-rtTA-M2* transgenic construct was microinjected into mouse embryonic stem cells by standard methods. Progeny were screened for incorporation of transgene by Southern blot and founder lines identified. Macrophage specific expression of rtTA was determined in mice transgenic for cfms-rtTA, tet-O-Cre and the ROSA26 LSL-lacZ allele [24]. cfms-rtTA mice were crossed with mice containing the NF-κB inhibiting $(tet\text{-}O)_7$-IκBαDN-Myc-His construct or the NF-κB activating $(tet\text{-}O)_7$-FLAG-cIKK2 construct [8, 10]. Double transgenics were termed DNFM or IKFM respectively. Littermates lacking one or both transgenes were used as controls.

To generate TG/Cre/FMR mice, Tomato Red/GFP reporter mice [25] were crossed with tet-O-Cre transgenic mice [26]. Double transgenic progeny were then crossed with cfms-rtTA mice to produce triple transgenic offspring containing all three transgenes. Littermates lacking the tet-O-Cre were used as controls.

Tail vein metastasis model

To induce transgene expression mice were treated with 2g/L dox (Sigma, St Louis, MO) in drinking water. Sucrose (5%) was added to decrease the bitter taste of dox water. A red bottle was used to prevent light-induced degradation and water was replaced twice weekly. For metastasis studies, 1 x 10^6 polyoma tumor cells (PyVT R221A or PYG 129) in PBS were injected via the tail vein. Mice were treated with dox either one week prior to cells until sacrifice, one week prior to cells until 2 days post injection, or 2 days post injection of cells until time of sacrifice. Mice were sacrificed at 2 weeks (PyVT R221A) or 5 weeks (PYG129) post cell injection for surface lung tumor quantification. Mouse lungs were inflated with Bouin's fixative (RICCA Chemical, Arlington, TX). After 24 hours of fixation, surface lung tumors were counted.

For seeding studies, mice were treated with dox for 1 week then 1 x 10^6 PyVT R221A tumor cells were injected via the tail vein. Mice were sacrificed 1 or 6 hours post cell injection and lungs harvested for Real-Time PCR and western blot analysis.

RNA isolation and RT-PCR

Tissue was homogenized in Trizol (Invitrogen, Carlsbad, CA) at sacrifice. For characterization, IKFM mice and controls were treated with dox for 1 week followed by IP injection of 1.5 ml of 4% thioglycolate in PBS. At sacrifice, three days post injection, the peritoneal cavity was lavaged with PBS and cells pelleted.

RNA isolation and reverse transcription reactions were performed as described [10] for all studies. For studies utilizing Real-Time PCR analysis, an Applied Biosystems Stepone Plus

Real-Time PCR system and SYBR Green PCR Master Mix (Applied Biosystems, Foster City, CA) were used. Primers: Polyoma middle T [27], TNF-α [10] , CXCL9: FOR 5' GTGGTGAAATAAAAAGATCAGGGC 3', REV 5' AAGAGAGAAATGGGTTCCCTG 3'; CCL3: FOR 5' TGCCCTTGCTGTTCTTCTCT 3', REV 5' GATGAATTGGCGTGGAATCT 3'; Mannose Receptor: FOR 5' CAAGGAAGGTTGGCATTTGT 3', REV 5' CCTTTCAGTCCTTTGCAAGC 3'; Arginase-1: FOR 5' ATGGAAGAGACCTTCAGCTAC 3', REV 5' GCTGTCTTCCCAAGAGTTGGG 3'; GAPDH: FOR 5' TGAGGACCAGGTTGTCTCCT 3', REV 5' CCCTGTTGCTGTAGCCGTAT 3'.

Bone marrow derived macrophages

IKFM and DNFM mice were treated with dox (2g/L) for 1 week and bone marrow-derived macrophages (BMDMs) isolated as described [28]. BMDMs were treated with dox (1 μg/ml) for 16 hours. RNA was isolated as above, and RT-PCR was completed with the following primers: IKK: FOR 5' GGAGCTCCACCGCGGTGCGG 3', REV 5' TCAGGGACATCTCGGGCAGC 3', and DN: FOR 5' CCTGGCTGTTGTCGAATACC-3', REV 5' GGT GATGGTGATGATGACCGG 3'. BMDMs were grown on microscope slides and treated with dox as above. Cells were fixed in 3% paraformaldehyde and stained for F4-80 (Invitrogen), with DAPI (Sigma).

Western blotting

Whole cell lung extracts were prepared and western blot performed as previously described [10]. Antibody: Cleaved-Caspase-3 (Cell Signaling Technology, Beverly, MA).

Luminol imaging

Mice were treated with dox (2g/L) for 1 week. L-012 (1.25 mg in 100 µl PBS, Wako Chemicals, Richmond, VA) was IV injected into anesthetized mice. Mice were imaged with an intensified charge-coupled device (ICCD) camera (IVIS 200; Xenogen, Hopkinton, MA). Light emission was detected as photon counts and analyzed by defining a standard area over the chest and determining total integrated photon intensity (Living Image software; Xenogen).

Flow Cytometry

Mice were sacrificed, lungs perfused with cold PBS, minced and incubated in RPMI media containing 0.7mg/ml collagenase XI (Sigma) and 30µg/ml DNAse I (Sigma) for 40 minutes at 37^{o}C. Digests were strained through a 70 micron filter. Cells were pelleted and treated with 1ml ACK red cell lysis buffer, washed, and re-suspended in PBS. Cells were blocked with anti-mouse CD16/CD32 antibody (eBioscience, San Diego, CA) before staining with anti-mouse antibodies: CD45 (30-F11), Gr-1 (Ly-6G), CD11b (M1/70), CD11c (N418), and CD19 (all eBioscience); F4/80 and B220 (Invitrogen); CD4 and NK1.1 (BD Pharmingen, San Diego, CA). Analysis was performed on an LSRII cytometer with DIVA software (BD Biosciences, Franklin Lakes, NJ).

CD11b positive cell isolation

Mice were treated with dox (2g/L) for one week prior to sacrifice. Lungs were digested as described above. Cell suspensions were incubated with MACS CDllb MicroBeads (Miltenyi Biotec, Auburn, CA) and separated by positive selection using MS columns.

Immunofluorescence (IF)

For whole lung tissue staining of IKFM and control mice, lungs were first perfused with PBS, then inflated and fixed in formalin overnight followed by paraffin embedding and sectioning. For cytospin staining, lungs were dissociated and CD11b+ cells positively selected as above. Cells were spun onto microscope slides then fixed in 3% paraformaldehyde. Antigen was unmasked by the sodium citrate method. Primary antibody: NF-κB phospho-p65 (Ser536) (Cell Signaling). Secondary antibody: goat anti-rabbit Alexa Fluor 594 (Invitrogen). DAPI (Sigma) was used for nuclei staining. Staining was visualized by Zeiss microscope and analyzed by MetaMorph software.

TG/Cre/FMR lungs were perfused with cold PBS and then inflated and fixed for 4-6 hours in 4% paraformaldehyde before being paraffin embedded and sectioned. DAPI (Sigma) counterstain was used as above.

Statistical analyses.

Statistical analyses were performed using Graph Pad Prism (GraphPad Software Inc., La Jolla, CA). All data are plotted graphically with vertical bars representing S.E. Unpaired Student's *t* test was used to assess differences between experimental conditions. A probability (*p*) value of < 0.05 was taken as an appropriate level of significance.

Results

Characterization of a novel transgenic model to activate or inhibit NF-κB activity in macrophages. To activate or inhibit NF-κB signaling in macrophages we used pairs of transgenics and the tet-on system. The first transgenic contains the Colony Stimulating Factor Receptor 1 promoter-reverse tetracycline transactivator (cfms-rtTA) leading to rtTA protein expression in macrophages. To generate IKFM mice, the cfms-rtTA is crossed with a transgenic containing the tet operon promoter element upstream of a FLAG-tagged constitutively activated human IKK2 (cIKK2) gene. For DNFM mice, the cfms-rtTA is crossed with a transgenic containing the tet operon promoter element upstream of a myc-tagged dominant negative IκBα (DN-IκBα) gene [8-10]. Treatment of IKFM or DNFM with dox results in expression of transgene in macrophages. Littermates lacking one or both transgenes were used as controls.

Bone marrow-derived macrophages (BMDMs) were cultured from IKFM or DNFM mice and controls. Immunohistochemistry for the macrophage specific marker F4/80 (Figure 1A, part i) and flow cytometry for both F4/80 and CD11b (Figure 1A, part ii) confirmed that the cells were macrophages. Cells were treated with dox (1μg/ml) for 24 hours, RNA isolated and reverse transcriptase polymerase chain reaction (RT-PCR) performed for the expression of cIKK2 mRNA or DN-IκBα mRNA. cIKK2 expression was observed in IKFM macrophages and DN-IκBα was observed in DNFM macrophages, with no transgene expression observed in controls (Figure 1A, part iii). Primers were designed such that the reverse primer was in the FLAG sequence (cIKK2) or myc sequence (DN-IκBα), ensuring specificity for transgene expression.

To test *in vivo* expression of transgene in macrophages, IKFM or control mice were treated with dox (2g/L) for 1 week. Thioglycolate-elicited peritoneal macrophages were isolated and RT-PCR performed for cIKK2 transgene expression. Transgene mRNA was expressed in

IKFM macrophages but not in controls (Figure 1B). To further characterize transgene expression *in vivo*, IKFM or control mice were treated with dox (2g/L) for 4 weeks. Tissues with high levels of macrophages were isolated and RT-PCR performed for expression of the cIKK2 transgene (Figure 1C). Transgene expression was observed in tissues from IKFM mice and was absent in controls. Equivalent characterization was completed in DNFM peritoneal macrophages and tissues that also demonstrated macrophage-targeted, inducible DN transgene expression.

To further determine both the macrophage cell specificity and the activity associated with the transgene expression, we utilized several methods. First, lungs from IKFM mice or controls treated with dox for 1 week were homogenized and CD11b positive and negative cells were separated. Using RT-PCR, cIKK2 expression was observed in CD11b positive cells from the lungs of IKFM mice but not in CD11b positive cells from control mice or in CD11b negative cells from IKFM mice (Figure 1D). Furthermore, equal numbers of CD11b positive cell populations from IKFM or control lungs were spun onto microscope slides and then stained and analyzed for nuclear phospho-p65 (Ser536). The CD11b positive cells isolated from IKFM lungs showed an almost 8 fold increase in the number of phospho-p65 positive macrophages vs. the number of positive macrophages in control CD11b positive cells (7.74 ± 0.95 fold increase, n=4 control and n=4 IKFM, $p = 0.0028$), indicating that cIKK2 transgene expression is indeed increasing NF-κB signaling.

To confirm the transgene's effect on NF-κB signaling *in vivo*, IKFM mice and controls were tail vein injected with PyVTR221A polyoma tumor cells. Mice were treated with dox beginning 2 days post injection until the time of sacrifice 2 weeks later, at which time all mice had similar lung tumor burden. Paraffin embedded tissue was sectioned and stained for phospho-p65 (Ser536) expression as an indicator of NF-κB activation. A subset of macrophages

within the IKFM lungs stained positive for nuclear phospho-p65, whereas none of these brightly stained macrophages were observed in control mice (Figure 1E). As an alternative approach to further confirm the cell specificity of the cfms-rtTA expression, we utilized a Tomato-Red/GFP reporter mouse crossed with a tet-O-Cre transgenic and the cfms-rtTA mouse. When treated with dox (2g/L), triple transgenic mice, termed TG/Cre/FMR, reveal which cells express the cfms-rtTA, as the rtTA/Cre combination within these cells flips the red fluorescence to green GFP. Sections of lung tissue from TG/Cre/FMR mice on dox for one week confirm that cells identified by morphology as macrophages are flipped to green (Figure 1F; No GFP positive cells were observed in control littermates which lacked the tet-O-Cre). Flow cytometry of lungs from TG/Cre/FMR mice and controls verifies that the GFP positive cells are $CD45^{+}CD11b^{+}$ and $Gr1^{-}$ (Figure 1F). GFP expression was undetectable in $CD45^{+}$ $Gr1^{+}$ $CD11b^{-}$ cells (data not shown).

Activation of NF-κB activity in macrophages leads to a reduction in tumor burden in a tail vein metastasis model. IKFM mice or controls were treated with dox for 1 week before injection of PyVT R221A cells. Dox treatment was continued until lungs were harvested 2 weeks post-cell injection. Analysis of surface lung tumor numbers revealed a significant reduction in lung tumors in IKFM mice as compared to controls (Figure 2A). The same experiment was performed in DNFM mice and controls, but no significant difference in lung tumor number was observed when NF-κB was inhibited (Figure 2B).

To investigate modulation of NF-κB during later stages of metastasis, PyVT R221A cells were injected in the tail vein of IKFM mice and controls and dox treatment was started 2 days *after* injection and continued until collection at 2 weeks post-injection. No significant difference was observed in tumor number between IKFM mice and controls (Figure 2C) suggesting that the

anti-tumor effect may be an earlier event. Additionally, DNFM mice were injected with PyVT R221A cells, and dox treatment was started 2 days *after* injection and continued until sacrifice. Upon collection, DNFM and control mice showed no significant difference in lung tumor number (control 67.00 ± 27.08, n=7; DNFM 45.44 ± 16.97, n=9, p = 0.4924;). Thus, in this model there is no evidence of a pro-metastatic phenotype mediated via NF-κB activity in macrophages from either IKFM or DNFM studies in which modulation occurs from 2 days post cell injection.

Reduction of lung metastasis by NF-κB in macrophages is an early event. As no effect was observed when dox treatment was started 2 days after cell injection, experiments were performed to look at the impact of NF-κB activation in macrophages in the period immediately surrounding tumor injection. IKFM mice and controls were treated with dox for 1 week before injection of PyVT R221A cells. Dox treatment was stopped 2 days post-injection and lungs were harvested 2 weeks post-injection. A significant reduction was observed in the number of lung tumors in IKFM compared to controls (Figure 3A). To ensure that this was not a cell line-specific effect, this experiment was repeated with a second, separately-derived mammary tumor cell line, PYG 129, that forms lung tumors 5 weeks after tail vein injection. IKFM mice and controls were treated with dox for 1 week before injection of PYG 129 cells via the tail vein. Dox treatment was stopped 2 days post-injection and lungs were harvested and surface tumors counted 5 weeks post-injection. A significant reduction in lung tumor formation was observed in IKFM mice as compared with control mice (Figure 3B). This indicates that the anti-tumor impact of NF-κB activation in macrophages occurs in the early stages of lung metastasis formation.

This experiment was repeated in DNFM mice to determine impact of NF-κB inhibition in macrophages on the early stages of lung metastasis formation. DNFM mice and controls were treated with dox for 1 week before injection of PyVT R221A cells. Dox treatment was stopped 2 days post-cell injection and lungs were harvested and surface tumors counted 2 weeks post-injection. A significant increase in tumor burden was observed in DNFM mice compared with controls (Figure 3C) confirming that NF-κB activity in macrophages blocks lung metastasis formation.

Activation of NF-κB in macrophages leads to a shift in macrophage populations in the lung. To assess the environment that the tumor cells encounter upon being injected into the IKFM mice, flow cytometric analysis was performed to look at macrophage populations in IKFM lungs compared with controls. Mice were treated with dox for 1 week, lungs were homogenized and CD45+ (leukocyte marker), F4/80+ (macrophage marker) cells were selected for further cell surface marker analysis. Three different cell populations were analyzed within this group: Gr1+/CD11b+ reported to represent immature myeloid cells including myeloid derived suppressor cells [29, 30], Gr1-/CD11b+ reported to represent newly recruited/mature macrophages [31] and Gr1-/CD11c+ which are reported to represent lung resident macrophages [32]. Although total F4/80 positive populations were not significantly different (Control 25.5 ± 13.3, IKFM 30.9 ± 2.8 n=4, p=0.45, percentages expressed out of total $CD45^+$ cells), a significant increase in the percentage of Gr1+/CD11b+ as well as Gr1-/CD11b+ cells was observed in IKFM as compared with control lungs. A significant decrease in Gr1-/CD11c+ cells was also observed in IKFM lungs (Figure 4). Thus, activation of NF-κB in macrophages correlates with a shift in the macrophage population surface markers in the lung environment that

suggests a population consisting of immature and recruited/mature cells with a lower proportion of resident lung macrophages even in the absence of tumor cells. A similar change in cell populations was observed in IKFM mice treated with dox for 1 week followed by cell injection and harvest of lungs two days post-injection. Therefore, this phenotype correlates with both time points at which a significant reduction in surface lung tumor formation was observed. A somewhat similar shift in monocyte populations is observed in control mice, but only *after* cell injection, whereas the changes occur in IKFM lungs with dox treatment alone. This suggests that activating NF-κB in macrophages "pre-educates" the IKFM lung environment to become anti-tumor, an effect that is achieved in control mice to a lesser degree only in response to tumor cells. These differences in macrophage populations were not observed in IKFM mice compared with controls when cells were injected, dox treatment started 2 days post-injection and lungs harvested for analysis 2 weeks post-injection, correlating with the lack of effect on lung tumor number. Analysis of markers of other immune cell types within the lungs after one week of dox treatment indicates that the percentages of $CD4^+$ T cells and $B220^+/CD19^+$ B cells are decreased in IKFM while the $NK1.1^+$ natural killer cell population is increased ($CD4^+$ T cells: control= 39.3± 2.6 and IKFM= 22.4 ± 0.7, $p = 0.0001$; $B220^+/CD19^+$ B cells: control= 15.1± 1.5 and IKFM= 10.1± 1.0, $p = 0.0123$; $NK1.1^+$ Natural Killer cells: control= 2.9± 0.4 and IKFM= 5.6± 0.5, $p = 0.0024$; n=6 control, n=8 IKFM for all markers and values expressed as percentage of $CD45^+$ cells). These changes are again suggestive of a pre-activated innate immune response that occurs prior to tumor cell injection.

Expression pattern in IKFM lung homogenates suggests that the majority of macrophages are M1 phenotype. To determine whether this reduction in lung metastases and alteration in

macrophage populations correlated with a particular macrophage phenotype, quantitative Real-Time PCR was performed for M1 and M2 markers. IKFM and controls were treated with dox for 1 week after which total lung RNA was extracted and Real-Time PCR performed. An increase was observed in CCL3 and TNF-α mRNA while a decrease was observed in Arginase-1 and Mannose Receptor mRNA (Figure 5). The decrease in Mannose Receptor expression was confirmed in CD11b positive cells isolated from IKFM vs. control lungs, assessed via Real-Time PCR (n=4 control, n=4 IKFM, $p = 0.003$). Taken together, this suggests that in the lungs of IKFM mice M1 represents the dominant macrophage phenotype [33].

A reduction in tumor cell seeding accompanied by an increase in apoptotic signaling is observed in lungs from IKFM mice. The effects on seeding of tumor cells after IV injection were investigated. IKFM and controls were treated with dox for one week before injection of PyVT R221A cells. Lungs were harvested at 1 hour and 6 hours post-injection and RNA isolated. Quantitative Real-Time PCR was performed for the Polyoma transgene which reflects tumor cell levels in the lungs. At 1 hour post-injection there was no significant difference in levels of Polyoma mRNA between control and IKFM (Figure 6A). At 6 hours post-injection a significant reduction in Polyoma mRNA was observed in IKFM lungs compared with control (Figure 6B). This suggests that there were less PyVT R221A cells in IKFM lungs than control at this point, perhaps due to an increased level of clearance, which would correlate with a lack of tumor formation in these mice.

To investigate whether the environment in IKFM lungs increased apoptosis of PyVT R221A cells, western blot for activated Caspase 3 was performed in whole lung homogenates. Caspase 3 activation was undetectable in the lungs of IKFM mice treated with dox for one week.

However, a higher level of Caspase 3 activation was observed in lungs from IKFM mice (Figure 6C) at 6 hours post cell injection indicating increased levels of apoptosis. This suggests that activation of NF-κB does not result in significant cell death in the absence of injected tumor cells and implies that the apoptosis occurs in the tumor cells as opposed to the lung epithelium.

Increased clearing of tumor cells and apoptosis in IKFM lungs correlates with higher ROS levels and increased CXCL9 expression. As an increased clearance of tumor cells had been observed, we were interested in the mechanism contributing to cytotoxic effects. Therefore, we investigated whether there was a change in levels of reactive oxygen species (ROS). IKFM mice and controls were treated with dox for 1 week and then injected with the L-012 luminol derivative to allow *in vivo* imaging of ROS levels over the chest area. IKFM mice showed a significant increase in ROS levels as compared with controls (Figure 6D). This suggests that the lung environment in IKFM mice was more cytotoxic to tumor cells correlating with increased clearance and a reduction in final tumor counts.

To further investigate the lung microenvironment at the time of tumor injection, cytokine profiling of bronchial alveolar lavage (BAL) fluid from IKFM mice and controls after 1 week of dox treatment was performed using the R&D Systems Proteome Profiler mouse cytokine panel array kit. The only significant difference detected was an increase in levels of CXCL9 (MIG) in the IKFM fluid (data not shown). To confirm this change, Real-Time PCR was performed on lung mRNA from the same time point. There was a significant increase in expression levels of CXCL9 (Figure 6E) which correlates with an anti-tumor environment [34].

Discussion

We generated a transgenic mouse model to investigate the role of classical NF-κB signaling in macrophages during tumorigenesis. We show that activation of NF-κB in macrophages in a mammary tumor tail vein metastasis model leads to a reduction in lung tumor formation with effects observed only when NF-κB is modulated prior to tumor cell introduction during the early seeding phase. Investigations into the lung phenotype associated with this effect show that activation of NF-κB leads to a shift in macrophage populations in the lung with a higher percentage of cells that are Gr1+/Cd11b+ and Gr1-/CD11b+ and a lower percentage of Gr1-/Cd11c+ cells. This shift in macrophage population and reduction in lung tumor numbers occurs in lungs that express increased levels of markers of the M1 anti-tumor macrophage phenotype. In agreement with this, we see a decrease in mammary tumor cell seeding following cell injection, an increase in apoptosis and enhanced formation of ROS and the cytokine CXCL9. Our data suggest that activation of NF-κB in macrophages within the lung during the seeding of lung metastases has an anti-tumor effect.

Our data is in contrast with other *in vivo* studies highlighting a tumor-promoting role for macrophages [17, 21]. This may be due to the different murine models and cancer types and the timing of NF-κB activation. These recently published studies have used the strategy of Cre-mediated deletion of the IKK2 to inhibit NF-κB signaling in myeloid cells. Our strategy employs specific activation of the signaling pathway by expression of a constitutive activator or direct inhibition by expression of a dominant form of inhibitor, either of which is regulated in an inducible manner. In our model, activation of NF-κB in macrophages before tumor cell arrival generates a hostile environment for tumor seeding and growth. This environment is similar to the M1-type macrophage response seen with a bacterial challenge [33]. The tail vein metastasis

model is inherently an acute model as mice develop a heavy metastatic load in the lungs at 2 weeks and need to be euthanized for humane reasons. This likely precludes observing the pro-tumor effects that have been reported in models of established tumors. Future studies to address effects on established tumors will need to be performed using orthotopic models or those in which spontaneous tumors arise, such as the polyoma transgenic model, to address this issue.

Recent studies highlight the complexity of NF-κB signaling during tumorigenesis. Tumor-associated macrophages isolated from an orthotopic fibrosarcoma model show a defective activation of NF-κB in response to LPS [16]. Further investigation reveals that this lack of activation is due to p50 subunit homodimers and knockout of p50 restores the M1 macrophage phenotype and reduces tumor burden [35]. While this study suggest that defective NF-κB activation within macrophages leads to the development of an M2, pro-tumor phenotype, others find that NF-kappaB signaling, specifically IKK2, is necessary to maintain the M2 phenotype in an ovarian cancer model [21]. These apparent contradictions were recently reviewed by Hagemann *et. al* [36] who propose that NF-κB regulation of TAM's is both context- and gene-dependent.

IKFM mice showed a significant shift in macrophage populations when NF-κB was activated for one week before tumors were established. Interestingly, when cells were analyzed at the third time point (where metastases are evident), a different pattern of surface marker expression was observed. This pattern was more similar to control populations. This agrees with recent reports showing the plasticity of the macrophage population during tumorigenesis with a different set of markers expressed at each stage [37].

The cell marker phenotype in the IKFM mice when an anti-tumor effect was observed correlates with the reduction in tumor burden. For example, GR1+/CD11b+ myeloid cells are a

source of ROS, the levels of which were seen to increase [29]. CXCL9 was significantly up-regulated in IKFM lungs after one week dox treatment. NF-κB activation leading to CXCL9 production within macrophages has previously been reported [38]. The injection of a mammary tumor cell line stably expressing CXCL9 cDNA into mice resulted in smaller tumors as well as fewer lung metastases. This was found to be a T-cell mediated effect, in that the CXCL9 overexpressing tumors had increased levels of infiltrating CD4 T cells as compared to vector controls [34]. Although we see increased CXCL9 expression in our model, we observed a concurrent decrease in CD4 T cells as assessed by flow cytometry. This could imply a separate, non-T-Cell-mediated, anti-tumor effect associated with CXCL9, or suggest that the time points analyzed were not optimal for analysis of lymphocyte infiltration. In either case, further investigation into the role of CXCL9 in this model is required.

Conclusions

We have generated a novel pair of transgenic models that enable NF-κB to be either activated or inhibited in an inducible manner in macrophages/monocytes by administration of dox in the drinking water. These models will enable investigations of the role of NF-κB within macrophages in defined temporal windows within tumor development and progression and will potentially be of use for investigations of other disease processes, such as atherosclerosis. In the current study the models have been used to investigate the effects of modulation of NF-κB during the seeding phase of metastasis. In contrast to what may have been predicted from the currently available literature, our data show that activation of NF-κB in a short, defined window inhibits metastasis. In addition, inhibition of NF-κB may actually contribute to increased metastasis. Given the recent interest in developing NF-κB inhibitors for clinical cancer therapy

[39] it is intriguing that, in our study, inhibition of NF-κB within macrophages during metastatic seeding resulted in a significant increase in lung tumor burden. This data suggests that inhibition in macrophages during tumorigenesis at certain time points may interfere with host-suppressive effects on metastasis formation, and demonstrates that timing and cell specificity may be the key determinants of the impact of NF-κB inhibitors as a cancer therapy.

Abbreviations

BAL: bronchoalveolar lavage; BMDMs: bone marrow derived macrophages; CCL3: Chemokine (C-C motif) ligand 3; CD11b: cluster of differentiation molecule 11B; cfms: colony stimulating factor -1 receptor promoter; cIKK2: constitutive form of inhibitor of nuclear factor kappa-B kinase subunit beta; CXCL9: Chemokine (C-X-C motif) ligand 9; DNFM: double transgenic mice which express dominant negative IKBα in macrophages in the presence of doxycycline; Dox: doxycycline; ICCD: intensified charge coupled device; IKBalphaDN: inhibitor of nuclear factor kappa B alpha dominant negative; IKFM: double transgenic mice which express cIKK2 in macrophages in the presence of doxycycline; IV: intravenous; IVIS: *in vivo* imaging system; LysM-cre: mouse strain expressing Cre recombinase from the endogenous *Lyzs* locus; MIG: monokine induced by gamma interferon; MMTV: mouse mammary tumor virus; NF-κB nuclear factor kappa B; PyVT: Polyoma middle T antigen mouse model; ROS: reactive oxygen species; RT-PCR: reverse transcriptase polymerase chain reaction; rtTA: reverse tetracycline transactivator; TAM: tumor associated macrophages; TNF-alpha: tumor necrosis factor alpha.

Competing interests

The authors declare that they have no competing interests.

Authors' contributions

LC performed initial characterization of the model, completed various trials of the tail vein studies, and drafted the manuscript. WB participated in ongoing breeding of the transgenic mice, completed tail vein trials and carried out Real-Time PCR, western-blot analysis and CDllb bead separation experiments. HO completed immunoflourescent staining, flow-cytometry

experiments and analysis, CDllb bead separation experiments – RT-PCR and IF, and carried out tail vein injections. LChen participated in the breeding, genotyping, treatment, and collection of mice. TS carried out tail vein injections and aided in lung analysis. TZ and MO created the cfms-rtTA transgenic mouse line. TB was involved in data interpretation and critically edited the manuscript. FE conceived of the study, participated in its design and coordination and helped draft the manuscript. All authors read and approved the final manuscript.

Acknowledgements

This study was supported by DOD Idea Award W81XWH-04-1-0456, DOD Concept Award W81XWH-09-1-0459 and NIH CA113734 (F.E. Yull) and the U.S. Department of Veterans Affairs (T. Blackwell.)

References

1. Mantovani A, Allavena P, Sica A, Balkwill F: **Cancer-related inflammation.** *Nature* 2008, **454:**436-444.
2. Mantovani A: **Molecular pathways linking inflammation and cancer.** *Curr Mol Med* 2010, **10:**369-373.
3. Ghosh S, May MJ, Kopp EB: **NF-kappa B and Rel proteins: evolutionarily conserved mediators of immune responses.** *Annu Rev Immunol* 1998, **16:**225-260.
4. Vallabhapurapu S, Karin M: **Regulation and function of NF-kappaB transcription factors in the immune system.** *Annu Rev Immunol* 2009, **27:**693-733.
5. Baeuerle PA, Baltimore D: **I kappa B: a specific inhibitor of the NF-kappa B transcription factor.** *Science* 1988, **242:**540-546.
6. Hayden MS, Ghosh S: **Shared principles in NF-kappaB signaling.** *Cell* 2008, **132:**344-362.
7. Baldwin AS, Jr.: **The NF-kappa B and I kappa B proteins: new discoveries and insights.** *Annu Rev Immunol* 1996, **14:**649-683.
8. Cheng DS, Han W, Chen SM, Sherrill TP, Chont M, Park GY, Sheller JR, Polosukhin VV, Christman JW, Yull FE, Blackwell TS: **Airway epithelium controls lung inflammation and injury through the NF-kappa B pathway.** *J Immunol* 2007, **178:**6504-6513.
9. Connelly L, Barham W, Onishko HM, Sherrill T, Chodosh LA, Blackwell TS, Yull FE: **Inhibition of NF-kappaB activity in mammary epithelium increases tumor latency and decreases tumor burden.** *Oncogene* 2010, **In press**.
10. Connelly L, Barham W, Pigg R, Saint-Jean L, Sherrill T, Cheng DS, Chodosh LA, Blackwell TS, Yull FE: **Activation of nuclear factor kappa B in mammary epithelium promotes milk loss during mammary development and infection.** *J Cell Physiol* 2010, **222:**73-81.
11. Pollard JW: **Tumour-educated macrophages promote tumour progression and metastasis.** *Nat Rev Cancer* 2004, **4:**71-78.
12. Coffelt SB, Hughes R, Lewis CE: **Tumor-associated macrophages: effectors of angiogenesis and tumor progression.** *Biochim Biophys Acta* 2009, **1796:**11-18.
13. Lewis CE, Pollard JW: **Distinct role of macrophages in different tumor microenvironments.** *Cancer Res* 2006, **66:**605-612.
14. Biswas SK, Sica A, Lewis CE: **Plasticity of macrophage function during tumor progression: regulation by distinct molecular mechanisms.** *J Immunol* 2008, **180:**2011-2017.
15. Allavena P, Sica A, Solinas G, Porta C, Mantovani A: **The inflammatory micro-environment in tumor progression: the role of tumor-associated macrophages.** *Crit Rev Oncol Hematol* 2008, **66:**1-9.
16. Biswas SK, Gangi L, Paul S, Schioppa T, Saccani A, Sironi M, Bottazzi B, Doni A, Vincenzo B, Pasqualini F, Vago L, Nebuloni M, Mantovani A, Sica A: **A distinct and unique transcriptional program expressed by tumor-associated macrophages (defective NF-kappaB and enhanced IRF-3/STAT1 activation).** *Blood* 2006, **107:**2112-2122.

17. Greten FR, Eckmann L, Greten TF, Park JM, Li ZW, Egan LJ, Kagnoff MF, Karin M: **IKKbeta links inflammation and tumorigenesis in a mouse model of colitis-associated cancer.** *Cell* 2004, **118:**285-296.
18. Maeda S, Kamata H, Luo JL, Leffert H, Karin M: **IKKbeta couples hepatocyte death to cytokine-driven compensatory proliferation that promotes chemical hepatocarcinogenesis.** *Cell* 2005, **121:**977-990.
19. Hagemann T, Wilson J, Burke F, Kulbe H, Li NF, Pluddemann A, Charles K, Gordon S, Balkwill FR: **Ovarian cancer cells polarize macrophages toward a tumor-associated phenotype.** *J Immunol* 2006, **176:**5023-5032.
20. Hagemann T, Wilson J, Kulbe H, Li NF, Leinster DA, Charles K, Klemm F, Pukrop T, Binder C, Balkwill FR: **Macrophages induce invasiveness of epithelial cancer cells via NF-kappa B and JNK.** *J Immunol* 2005, **175:**1197-1205.
21. Hagemann T, Lawrence T, McNeish I, Charles KA, Kulbe H, Thompson RG, Robinson SC, Balkwill FR: **"Re-educating" tumor-associated macrophages by targeting NF-kappaB.** *J Exp Med* 2008, **205:**1261-1268.
22. Martin MD, Fingleton B, Lynch CC, Wells S, McIntyre JO, Piston DW, Matrisian LM: **Establishment and quantitative imaging of a 3D lung organotypic model of mammary tumor outgrowth.** *Clin Exp Metastasis* 2008, **25:**877-885.
23. Sasmono RT, Oceandy D, Pollard JW, Tong W, Pavli P, Wainwright BJ, Ostrowski MC, Himes SR, Hume DA: **A macrophage colony-stimulating factor receptor-green fluorescent protein transgene is expressed throughout the mononuclear phagocyte system of the mouse.** *Blood* 2003, **101:**1155-1163.
24. Soriano P: **Generalized lacZ expression with the ROSA26 Cre reporter strain.** *Nat Genet* 1999, **21:**70-71.
25. Muzumdar MD, Tasic B, Miyamichi K, Li L, Luo L: **A global double-fluorescent Cre reporter mouse.** *Genesis* 2007, **45:**593-605.
26. Perl AK, Wert SE, Nagy A, Lobe CG, Whitsett JA: **Early restriction of peripheral and proximal cell lineages during formation of the lung.** *Proc Natl Acad Sci U S A* 2002, **99:**10482-10487.
27. Yee KO, Connolly CM, Duquette M, Kazerounian S, Washington R, Lawler J: **The effect of thrombospondin-1 on breast cancer metastasis.** *Breast Cancer Res Treat* 2009, **114:**85-96.
28. Connelly L, Jacobs AT, Palacios-Callender M, Moncada S, Hobbs AJ: **Macrophage endothelial nitric-oxide synthase autoregulates cellular activation and pro-inflammatory protein expression.** *J Biol Chem* 2003, **278:**26480-26487.
29. Kusmartsev S, Gabrilovich DI: **Effect of tumor-derived cytokines and growth factors on differentiation and immune suppressive features of myeloid cells in cancer.** *Cancer Metastasis Rev* 2006, **25:**323-331.
30. Ostrand-Rosenberg S, Sinha P: **Myeloid-derived suppressor cells: linking inflammation and cancer.** *J Immunol* 2009, **182:**4499-4506.
31. Mosser DM, Edwards JP: **Exploring the full spectrum of macrophage activation.** *Nat Rev Immunol* 2008, **8:**958-969.
32. Gonzalez-Juarrero M, Shim TS, Kipnis A, Junqueira-Kipnis AP, Orme IM: **Dynamics of macrophage cell populations during murine pulmonary tuberculosis.** *J Immunol* 2003, **171:**3128-3135.

33. Benoit M, Desnues B, Mege JL: **Macrophage polarization in bacterial infections.** *J Immunol* 2008, **181:**3733-3739.
34. Walser TC, Ma X, Kundu N, Dorsey R, Goloubeva O, Fulton AM: **Immune-mediated modulation of breast cancer growth and metastasis by the chemokine Mig (CXCL9) in a murine model.** *J Immunother* 2007, **30:**490-498.
35. Saccani A, Schioppa T, Porta C, Biswas SK, Nebuloni M, Vago L, Bottazzi B, Colombo MP, Mantovani A, Sica A: **p50 nuclear factor-kappaB overexpression in tumor-associated macrophages inhibits M1 inflammatory responses and antitumor resistance.** *Cancer Res* 2006, **66:**11432-11440.
36. Hagemann T, Biswas SK, Lawrence T, Sica A, Lewis CE: **Regulation of macrophage function in tumors: the multifaceted role of NF-kappaB.** *Blood* 2009, **113:**3139-3146.
37. Qian BZ, Pollard JW: **Macrophage diversity enhances tumor progression and metastasis.** *Cell* 2010, **141:**39-51.
38. Powell JD, Boodoo S, Horton MR: **Identification of the molecular mechanism by which TLR ligation and IFN-gamma synergize to induce MIG.** *Clin Dev Immunol* 2004, **11:**77-85.
39. Lin Y, Bai L, Chen W, Xu S: **The NF-kappaB activation pathways, emerging molecular targets for cancer prevention and therapy.** *Expert Opin Ther Targets* 2010, **14:**45-55.

Figure Legends

Figure 1. Characterization of IKFM and DNFM mouse models. A. Bone marrow derived macrophages were isolated from IKFM and DNFM mice and i) stained for F4/80 via immunofluorescent staining (green= F4/80 and blue=DAPI), ii) subjected to flow cytometric analysis of F4/80 and CD11b and iii) treated with 1µg/ml dox for 24hrs *in vitro* and gene expression analyzed via RT-PCR. B. Peritoneal macrophages were isolated from 1 week dox treated (2g/L) IKFM mice and transgene expression analyzed via RT-PCR. C. IKFM mice and controls were treated with dox (2g/L) for 4 weeks and transgene expression was detected by RT-PCR in lung, liver, intestines (Int), and bone marrow (BM). D. IKFM and control mice were treated with dox (2g/L) for one week and CD11b positive and negative populations isolated from lungs for RT-PCR analysis of IKK. GAPDH was performed as control. E. Phospho-p65 (Ser536) immunoflourescent staining (red= phospho-p65 and blue= DAPI) of lungs from IKFM and control mice bearing lung metastasis and treated with dox (2g/L). F. i) Lung sections of TG/Cre/FMR mice treated with dox for one week (blue=DAPI) and ii) flow analysis of TG/Cre/FMR and control lungs. Total cells were first sorted for CD45 and CD11b double positive cells. This double positive population was then further sorted for Gr-1 and GFP, as shown.

Figure 2. Activation of NF-κB in macrophages results in fewer lung metastasis. IKFM or DNFM mice and controls were treated with dox (2g/L) for one week prior to PyVT cell injection. Dox treatment was continued until sacrifice at 2 weeks post-injection. A. Lung tumor counts in IKFM and control mice ($p=0.0005$; n=11 control, n=8 IKFM) and representative lung images. B. Lung tumor counts in DNFM and control mice ($p=0.7997$; n=6 control, n=8 DNFM).

C. IKFM mice were injected with PyVT cells. Dox treatment (2g/L) began 2 days post injection and continued until sacrifice at 2 weeks post cells when surface lung tumors were counted ($p=0.9880$; n=7 control, n=6 IKFM).

Figure 3. Reduction of lung metastasis by NF-κB in macrophages is an early event. IKFM or DNFM mice and controls were treated with dox (2g/L) for one week prior to cell injection. Dox treatment ended 2 days post cell injection and mice were sacrificed at 2 weeks post cells (PyVT R221A) or 5 weeks post cells (PYG 129). A. Lung tumor counts in IKFM injected with PyVT R221A cells ($p<0.0001$; n=10 control, n=7 IKFM) and representative lung images. B. Lung tumor counts in IKFM injected with PYG 129 cells ($p=0.0270$; n=9 control, n=8 IKFM). C. Lung tumor counts in DNFM injected with PyVT R221A cells ($p=0.0039$; n=6 control, n=9 DNFM).

Figure 4. Activation of NF-κB in macrophages leads to a shift in macrophage populations in the lung. Flow cytometric analysis of dissociated lung cells from IKFM and control mice. 3 treatment groups (all 2g/L dox): 1 wk dox – mice were on dox for 1 week (control n=4, IKFM n=4); 2 days dox – mice were on dox for 1 week, PyVT R221A cells were injected via tail vein, dox treatment was stopped 2 days after injection and mice sacrificed (control n=3, IKFM n=4); 2 wks dox – mice were injected with PyVT cells via tail vein, 2 days later mice were put on dox and 2 weeks after cell injection mice were sacrificed (control n=3, IKFM n=3). All cells were gated for CD45+ and then for F4/80+ cells. A. Representative flow diagrams of 1 wk dox treatment group. Graphs (B) and table (C) showing percentage of cell populations that were

Gr1+/CD11b+ (black), Gr1-/CD11b+ (grey) and Gr1-/Cd11c+ (white; *$p < 0.05$, **$p < 0.01$, ***$p < 0.001$; $n \geq 3$ for all groups).

Figure 5. Expression pattern in IKFM lung homogenates suggests that the majority of macrophages are M1 phenotype. RNA was isolated from whole lung samples of IKFM and control mice treated with dox (2g/L) for one week. Quantitative real time PCR was performed for A. CCL3, B. Mannose receptor, C. Arginase-1 and D. TNF-alpha ($p < 0.05$, **$p < 0.01$, ***$p < 0.001$; n=5 control, n=5 IKFM).

Figure 6. A reduction in tumor cell seeding is observed in lungs from IKFM mice. IKFM and control mice were treated with dox (2g/L) for one week before injection of PyVT R221A cells. Lungs were harvested at 1 hour (A, n=5 control, n=7 IKFM, p=0.4410) and 6 hours (B, n=3 control, n=3 IKFM, p=0.0214) post injection and RNA isolated from whole lung samples for quantitative real time PCR analysis of Polyoma (PYL) expression B. Western blot for cleaved caspase-3 on whole cell lung homogenates from mice treated with dox for one week (no cells injected) (n=4 control and n=4 IKFM) and homogenates from the 6 hour time point (n=4 control and n=4 IKFM) C. IKFM mice and controls were treated with dox for one week and then imaged for ROS (n=3 control and n=3 IKFM; p= 0.0011). E. Real time PCR analysis of whole lung RNA for CXCL9 (n=4 control, n=3 IKFM, p=0.0033).

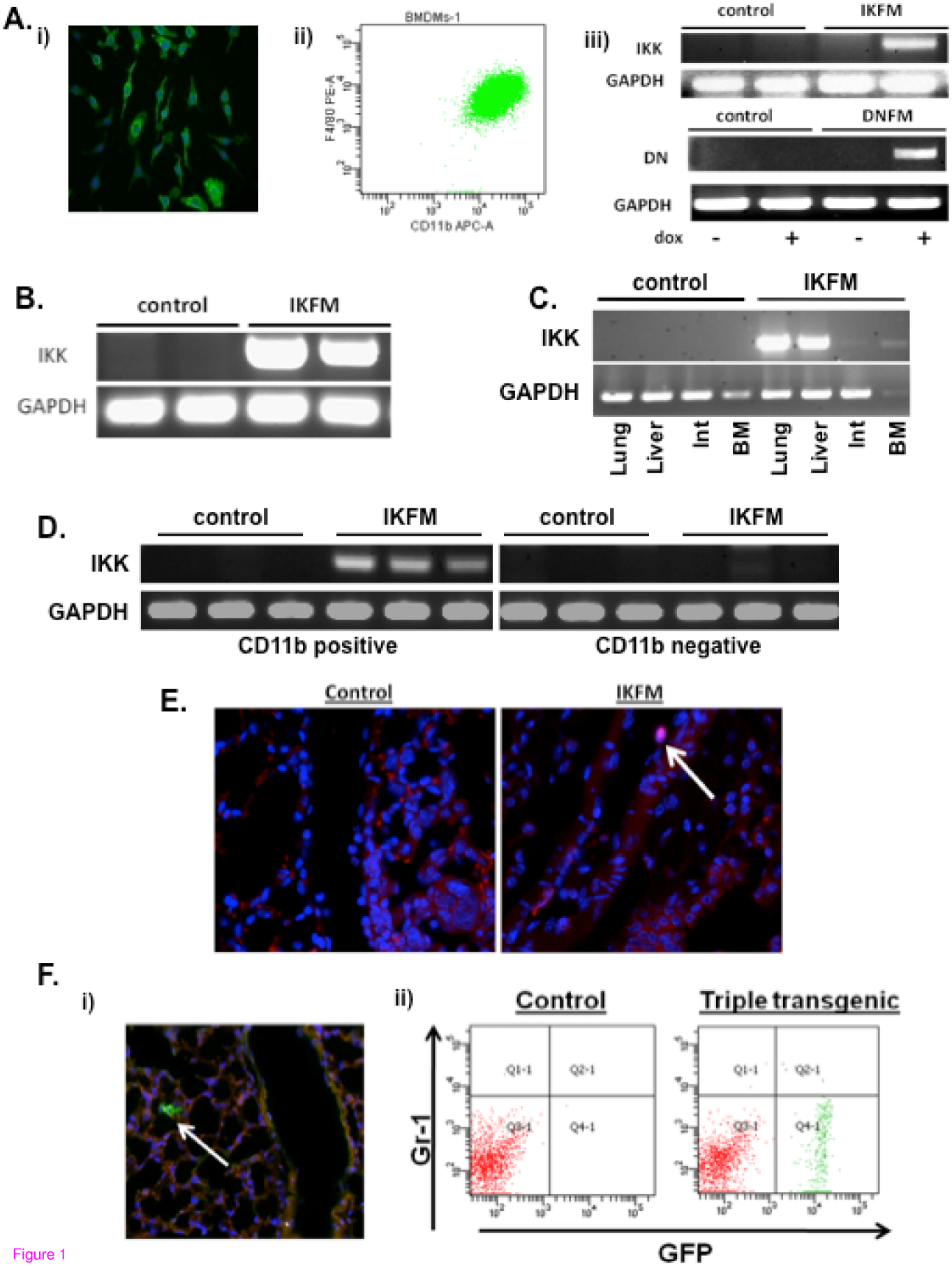
A.
i)
ii)
BMDMs-1
F4/80 PE-A
CD11b APC-A
iii)
control
IKFM
IKK
GAPDH
control
DNFM
DN
GAPDH
dox - + - +
B.
control
IKFM
IKK
GAPDH
C.
control
IKFM
IKK
GAPDH
Lung
Liver
Int
BM
Lung
Liver
Int
BM
D.
control
IKFM
control
IKFM
IKK
GAPDH
CD11b positive
CD11b negative
E.
Control
IKFM
F.
i)
ii)
Control
Triple transgenic
Gr-1
GFP
Q1-1
Q2-1
Q3-1
Q4-1

Figure 1

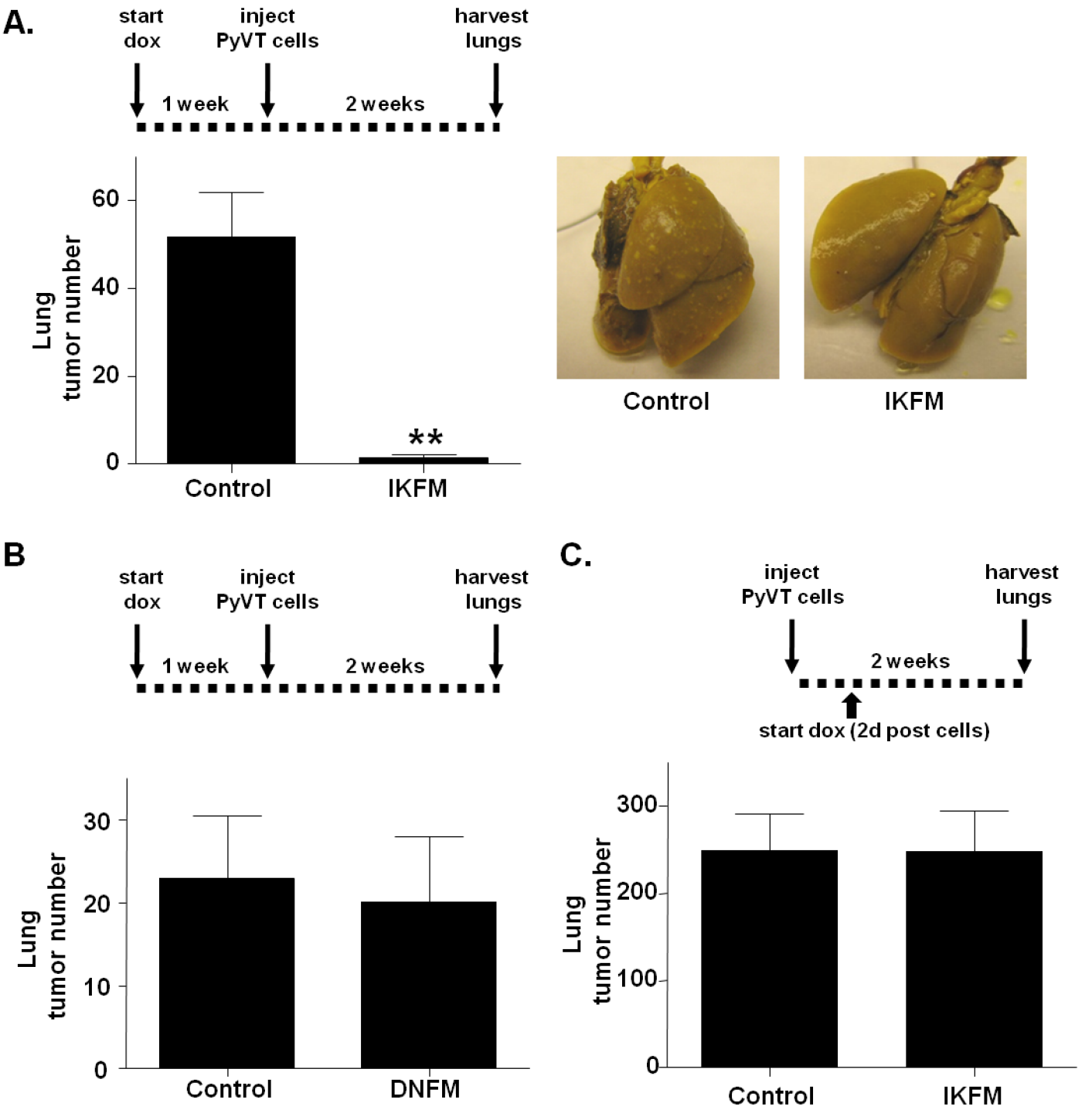
A.
start dox
inject PyVT cells
harvest lungs
1 week
2 weeks
Lung tumor number
60
40
20
0
**
Control
IKFM
Control
IKFM
B
start dox
inject PyVT cells
harvest lungs
1 week
2 weeks
Lung tumor number
30
20
10
0
Control
DNFM
C.
inject PyVT cells
harvest lungs
2 weeks
start dox (2d post cells)
Lung tumor number
300
200
100
0
Control
IKFM

Figure 2

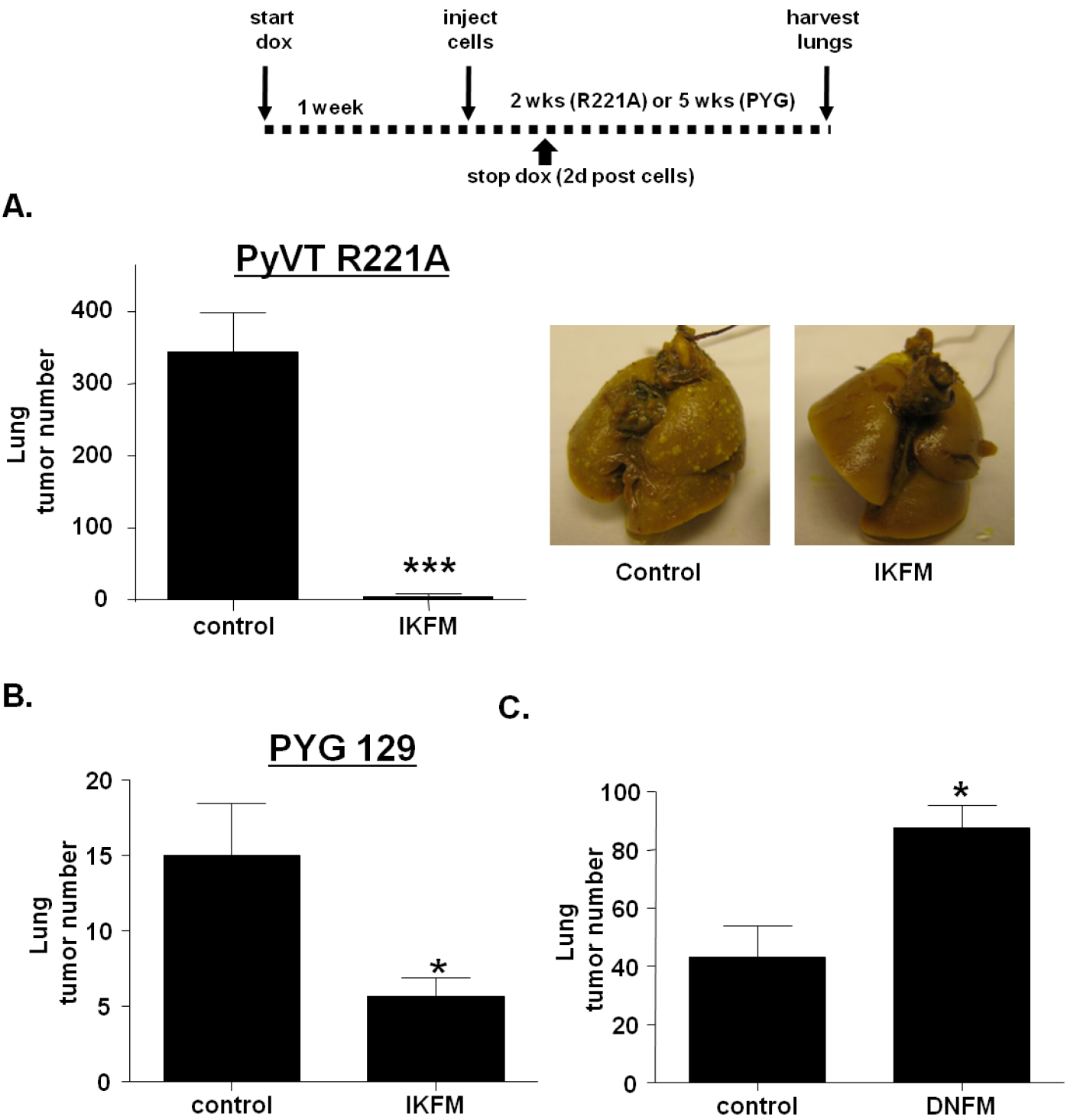
start dox
inject cells
harvest lungs
1 week
2 wks (R221A) or 5 wks (PYG)
stop dox (2d post cells)
A.
PyVT R221A
Lung tumor number
400
300
200
100
0
***
control
IKFM
Control
IKFM
B.
PYG 129
Lung tumor number
20
15
10
5
0
*
control
IKFM
C.
Lung tumor number
100
80
60
40
20
0
*
control
DNFM

Figure 3

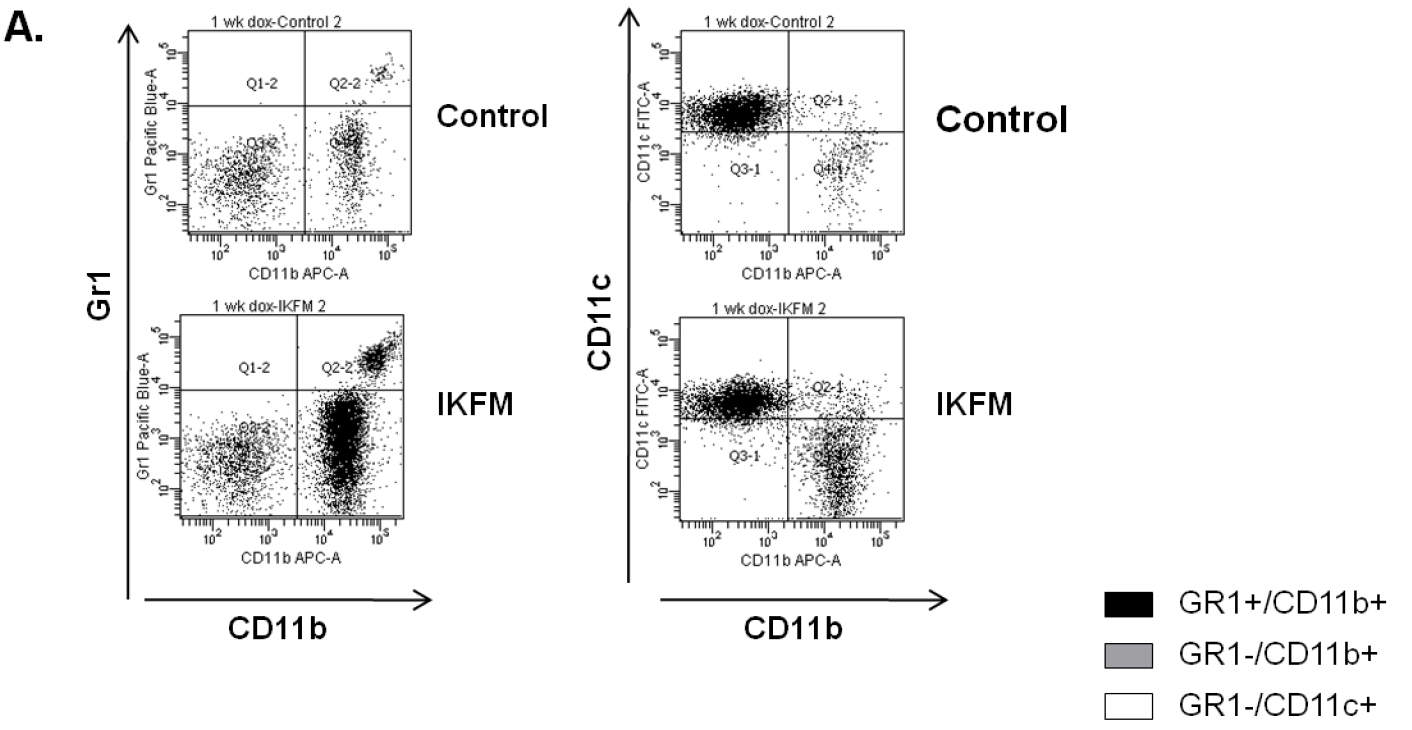

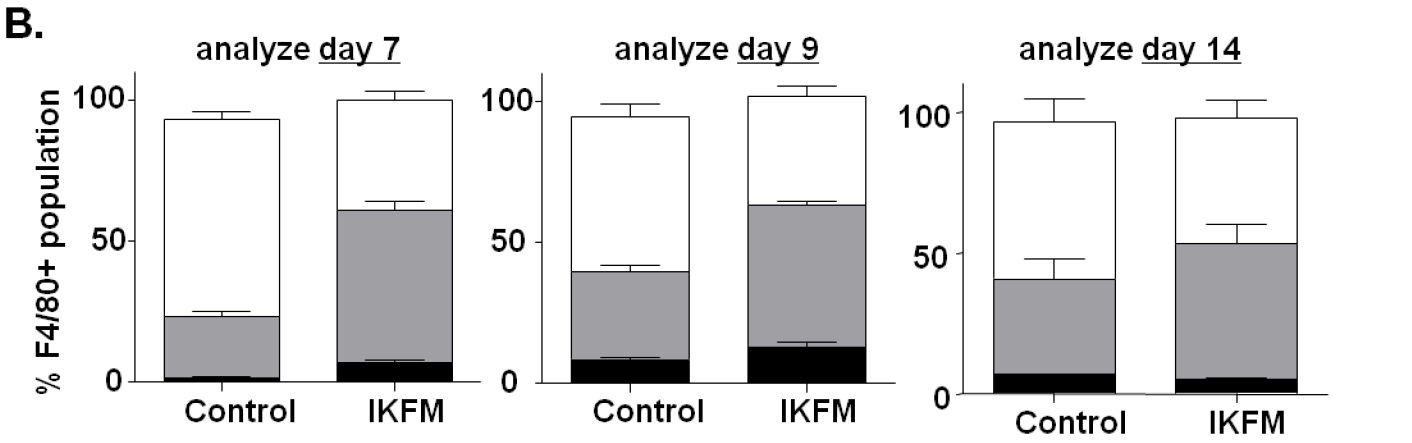

C.

		% F4-80+ population		
Condition	Group	Gr1+/CD11b+	Gr1-/CD11b+	Gr1-/CD11c+
• day 0 = start dox • analyze day 7 (no cells)	Control	1.4 ± 0.2	21.7 ± 2.1	69.9 ± 2.7
	IKFM	6.7 ± 1.3 **	54.3 ± 3.0 ***	38.3 ± 3.4 ***
• day 0 = start dox • day 7 = cells • analyze day 9	Control	8.4 ± 0.7	30.9 ± 2.6	55.1 ± 4.5
	IKFM	12.8 ± 1.5	50.4 ± 1.2 ***	38.3 ± 3.7 *
• day 0 = cells • day 2 = start dox • analyze day 14	Control	6.8 ± 0.3	34.0 ± 7.0	55.6 ± 8.1
	IKFM	5.0 ± 0.5 *	48.4 ± 6.7	44.4 ± 6.5

Figure 4

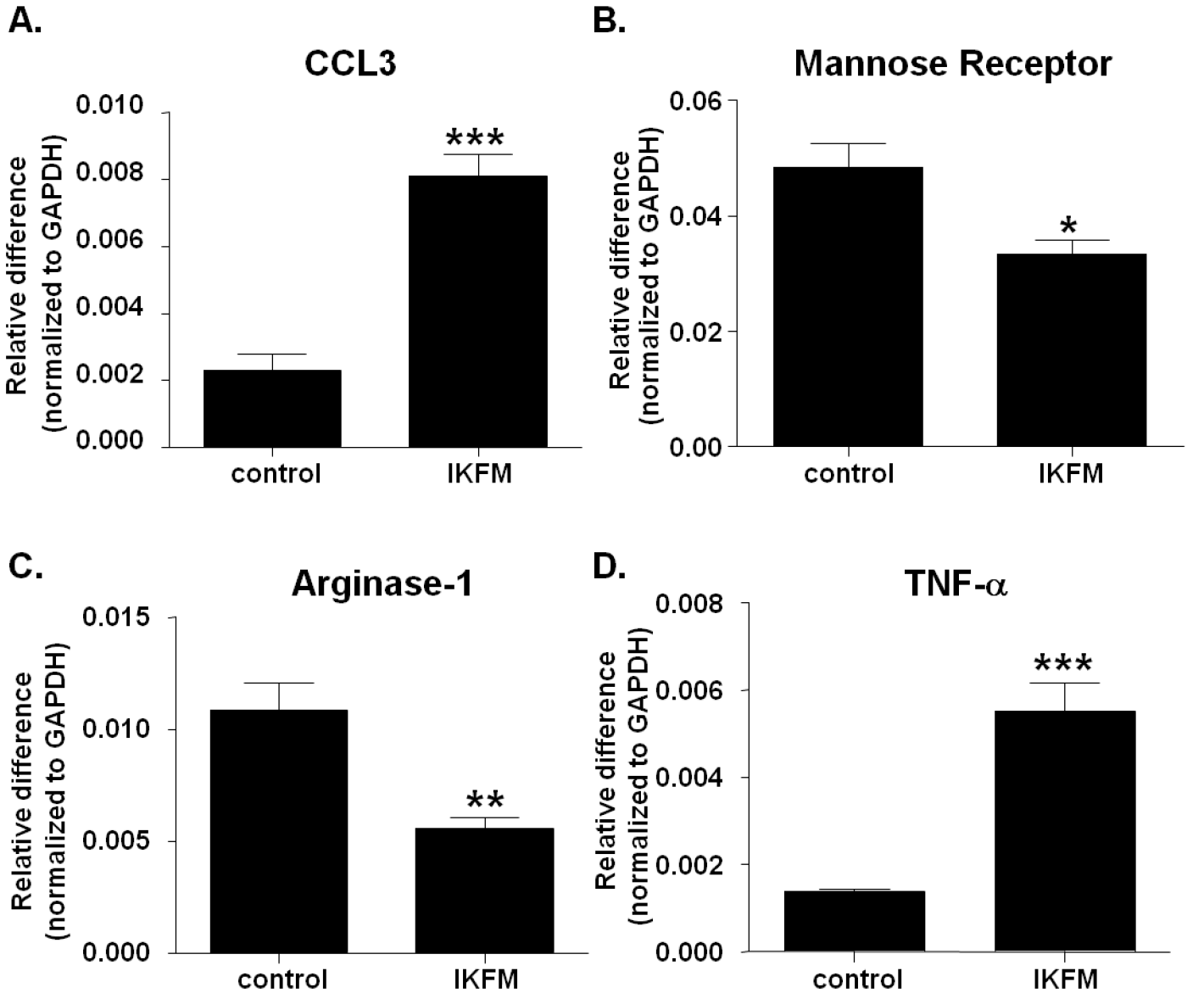
A.
CCL3
Relative difference (normalized to GAPDH)
0.010
0.008
0.006
0.004
0.002
0.000
***
control
IKFM
B.
Mannose Receptor
Relative difference (normalized to GAPDH)
0.06
0.04
0.02
0.00
*
control
IKFM
C.
Arginase-1
Relative difference (normalized to GAPDH)
0.015
0.010
0.005
0.000
**
control
IKFM
D.
TNF-α
Relative difference (normalized to GAPDH)
0.008
0.006
0.004
0.002
0.000
***
control
IKFM

Figure 5

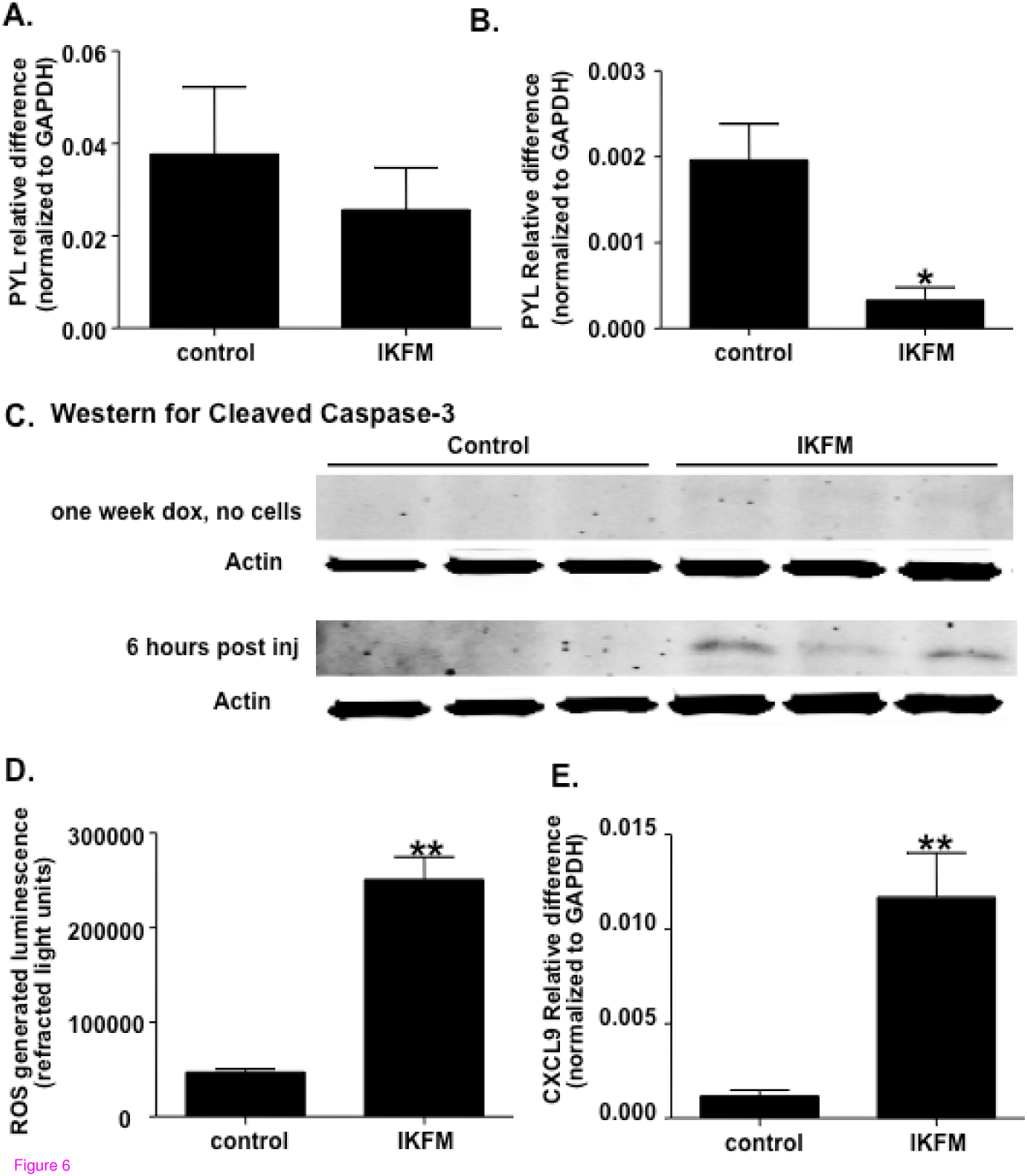
A.
PYL relative difference (normalized to GAPDH)
0.06
0.04
0.02
0.00
control
IKFM
B.
PYL Relative difference (normalized to GAPDH)
0.003
0.002
0.001
0.000
*
control
IKFM
C. Western for Cleaved Caspase-3
Control
IKFM
one week dox, no cells
Actin
6 hours post inj
Actin
D.
ROS generated luminescence (refracted light units)
300000
200000
100000
0
**
control
IKFM
E.
CXCL9 Relative difference (normalized to GAPDH)
0.015
0.010
0.005
0.000
**
control
IKFM

Figure 6

THE JOURNAL OF IMMUNOLOGY

NF-κB Signaling in Fetal Lung Macrophages Disrupts Airway Morphogenesis

Timothy S. Blackwell, Ashley N. Hipps, Yasutoshi Yamamoto, Wei Han, Whitney J. Barham, Michael C. Ostrowski, Fiona E. Yull and Lawrence S. Prince

J Immunol 2011;187;2740-2747; Prepublished online 20 July 2011;
doi:10.4049/jimmunol.1101495
http://www.jimmunol.org/content/187/5/2740

The Journal of Immunology is published twice each month by The American Association of Immunologists, Inc., 9650 Rockville Pike, Bethesda, MD 20814-3994.

Print ISSN: 0022-1767 Online ISSN: 1550-6606.

NF-κB Signaling in Fetal Lung Macrophages Disrupts Airway Morphogenesis

Timothy S. Blackwell,*,†,‡,§ Ashley N. Hipps,†,¶ Yasutoshi Yamamoto,¶ Wei Han,* Whitney J. Barham,‡ Michael C. Ostrowski,‖ Fiona E. Yull,‡ and Lawrence S. Prince†,¶

Bronchopulmonary dysplasia is a common pulmonary complication of extreme prematurity. Arrested lung development leads to bronchopulmonary dysplasia, but the molecular pathways that cause this arrest are unclear. Lung injury and inflammation increase disease risk, but the cellular site of the inflammatory response and the potential role of localized inflammatory signaling in inhibiting lung morphogenesis are not known. In this study, we show that tissue macrophages present in the fetal mouse lung mediate the inflammatory response to LPS and that macrophage activation inhibits airway morphogenesis. Macrophage depletion or targeted inactivation of the NF-κB signaling pathway protected airway branching in cultured lung explants from the effects of LPS. Macrophages also appear to be the primary cellular site of IL-1β production following LPS exposure. Conversely, targeted NF-κB activation in transgenic macrophages was sufficient to inhibit airway morphogenesis. Macrophage activation in vivo inhibited expression of multiple genes critical for normal lung development, leading to thickened lung interstitium, reduced airway branching, and perinatal death. We propose that fetal lung macrophage activation contributes to bronchopulmonary dysplasia by generating a localized inflammatory response that disrupts developmental signals critical for lung formation. ***The Journal of Immunology*****, 2011, 187: 2740–2747.**

During fetal lung morphogenesis, simple epithelial tubes develop into a complex structure competent for gas exchange (1, 2). This process fails to occur normally in preterm infants with bronchopulmonary dysplasia (BPD), a chronic disease that affects ~60% of preterm infants born before 28 wk (3). BPD results from arrested airway morphogenesis during the canalicular and saccular stages of lung development. Normally during these stages, small terminal airways branch, expand, and divide to form alveolar ducts. In patients with BPD, arrested development leads to fewer saccular stage airways, reduced numbers of alveoli, and lower capacity for gas exchange (4). Infants born after the early saccular stage of development rarely develop BPD, suggesting that the canalicular and early saccular stages represent a window of disease susceptibility. Various environmental factors have been implicated in development of BPD, involving either airway epithelial injury or lung inflammation (5, 6). Understanding how these factors lead to arrested airway morphogenesis will be critical for developing new therapeutic approaches.

Several lines of clinical and experimental evidence suggest infection or injury leads to an inflammatory response that causes or exacerbates BPD. First, chorioamnionitis (infection and inflammation of the amniotic membranes) is detected in up to 70% of preterm deliveries and is associated with increased BPD risk (7). Second, infants that develop BPD often have elevated levels of inflammatory mediators in their airway both at birth and during the later stages of disease progression (8, 9). Third, injecting *Escherichia coli* LPS into the amniotic fluid of pregnant animals inhibits airway branching and prevents subsequent alveolar development (10, 11). In developing an experimental mouse model for studying the mechanisms leading to BPD, we observed that LPS prevents saccular airway branching in both fetal mice and cultured fetal mouse lung explants. These data suggest innate immune activation and inflammatory signaling intersect with developmental pathways, interfering with processes required for branching morphogenesis.

LPS can inhibit airway branching in fetal lung explants in the absence of circulating inflammatory cells (10), suggesting that resident lung cells are competent to transduce signals that interrupt normal lung development. We have previously identified multiple gene targets of inflammatory signaling that are critical for normal airway morphogenesis (9, 12–14). However, the cellular site of the initial innate immune response critical for disrupting development is not known. Among the cell types in the fetal lung, airway epithelia and vascular endothelia appear at least somewhat capable of responding to microbial products (15, 16). To date, the potential role of macrophages in the fetal lung innate immune response has not been closely examined. Studies involving fetal macrophages have focused primarily on their ability to remove apoptotic cellular debris and remodel extracellular matrix (17–19). In this study, we report that macrophages are the primary cellular sites of the fetal lung innate immune response. Macrophage

*Department of Medicine, Vanderbilt University School of Medicine, Nashville, TN 37232; †Department of Cell and Developmental Biology, Vanderbilt University School of Medicine, Nashville, TN 37232; ‡Department of Cancer Biology, Vanderbilt University School of Medicine, Nashville, TN 37232; §Department of Veterans Affairs Medical Center, Nashville, TN 37212; ¶Department of Pediatrics, Vanderbilt University School of Medicine, Nashville, TN 37232; and ‖Department of Molecular and Cellular Biochemistry, The Ohio State University, Columbus, OH 43210

Received for publication May 25, 2011. Accepted for publication June 29, 2011.

This work was supported by the Department of Veterans Affairs (to T.S.B.), National Institutes of Health Grants AI079253 (to T.S.B.), HL097195 (to L.S.P. and T.S.B.), HL086324 (to L.S.P), CA113734 (to F.E.Y.), and HL069765 (to A.N.H.), and Department of Defense Concept Award W81XWH-09-1-0459 (to F.E.Y.). Confocal imaging was performed in part through the use of the Vanderbilt University Medical Center Cell Imaging Shared Resource (supported by National Institutes of Health Grants CA68485, DK20593, DK58404, HD15052, DK59637, and EY08126).

Address correspondence and reprint requests to Dr. Lawrence S. Prince, Division of Neonatology, Departments of Pediatrics and Cell and Developmental Biology, Vanderbilt University School of Medicine, 9435A MRBIV, 2213 Garland Avenue, Nashville, TN 37232. E-mail address: lawrence.s.prince@vanderbilt.edu

The online version of this article contains supplemental material.

Abbreviations used in this article: BPD, bronchopulmonary dysplasia; cIKKβ, constitutively active IκB kinase β mutant; E, embryonal day; FGF-10, fibroblast growth factor-10; IKKβ, IκB kinase β; IKKβΔ, LysM-Cre:IKKβ$^{f/f}$ mice.

www.jimmunol.org/cgi/doi/10.4049/jimmunol.1101495

activation is required for the LPS-mediated production of inflammatory mediators that disrupt airway branching. In addition, targeted activation of fetal lung macrophages, both in cultured lung explants and developing mouse lungs in vivo, inhibits airway morphogenesis and produces a lung phenotype that closely resembles human BPD. Our findings indicate that macrophage activation and subsequent lung inflammation may play a key role in BPD pathogenesis.

Materials and Methods

Reagents

Gel-purified *E. coli* LPS (O55:B5) was purchased from Sigma-Aldrich. The following Abs were used for immunolabeling: rat anti-CD68 (Acris), rat anti-F4/80 (Acris), rat anti–E-cadherin (Zymed), rabbit anti-CD14 (Santa Cruz Biotechnology), and rabbit anti-GFP (Abcam). DAPI, TO-PRO-3 iodide, ProLong Gold antifade reagent with DAPI, and Alexa-conjugated secondary Abs were purchased from Invitrogen. Anti-CD11b Microbeads and magnetic separation equipment and reagents were purchased from Miltenyi Biotec. Reagents for preparing liposomal clodronate were obtained from Sigma-Aldrich. All cell culture media were purchased from Invitrogen. FBS was purchased from Thermo Fisher Scientific.

Mouse strains and lung explant culture

All animal experiments were thoroughly reviewed and approved by the Vanderbilt University Institutional Animal Care and Use Committee. BALB/cJ and Rosa26-YFP mice were obtained from The Jackson Laboratory. NGL (20), LysM-Cre:IKK$\beta^{F/F}$ (21), and IKFM (L. Connelly, W. Barham, H.M. Onishko, L. Chen, T. Sherrill, T. Zabuawala, M.C. Ostrowski, T.S. Blackwell, and F.E. Yull, submitted for publication) mouse strains were developed and described previously. For timed pregnant matings, embryonal day 0 (E0) was defined as the morning of vaginal plug discovery. To induce transgene expression in IKFM mice, timed pregnant dams were given doxycycline-containing water (2 g/l) ad libitum. E15 fetal mouse lung explants were isolated and cultured as previously described (16). For transgenic models, lungs of each mouse embryo were minced and cultured separately. Approximately 20 explants were isolated from each embryo. All explants studied were between 0.8 and 1.2 mm in diameter at initial time of culture. To quantify saccular airway branching in cultured lung explants, brightfield images of explants were acquired every 24 h of culture. Airway branching was expressed as the number of new branches that formed between 24 and 72 h of culture in each explant. For macrophage depletion using clodronate, control or clondronate-containing liposomes were directly added to explants at the initial time of isolation. LPS was then added to the media 24 h later.

Fetal lung macrophage isolation

E15 fetal mouse lungs were dissected free of surrounding tissues and placed in ice-cold PBS. The lungs were homogenized and forced through 100-μm and 40-μm cell strainers. Cells were pelleted by centrifugation and resuspended in the presence of anti-CD11b–conjugated Microbeads (Miltenyi Biotec). The CD11b-labeled cells were collected using a magnetic separator, washed, and plated in RPMI 1640 with 10% FBS. Following overnight culture at 37˚C in 95% air/5% CO_2, macrophages were washed and treated for 4 h with LPS (250 ng/ml). NGL macrophages were similarly isolated, treated with LPS for various time points, and solubilized in Reporter Lysis Buffer (Promega). Luciferase activity was measured using SteadyGlo reagent (Promega) and a Synergy HT microplate reader (Biotek). Luciferase activity was normalized to total protein content as measured by BCA assay (Promega).

RNA isolation, real-time PCR, and IL-1β measurement

Total RNA isolation, cDNA synthesis, and real-time PCR were performed using standard techniques. Gene expression was compared using the $2^{-\Delta\Delta CT}$ method. Independent experiments were performed at least three separate times. Data between groups were compared by ANOVA or Student *t* test to test for significant differences. IL-1β concentrations were measured in homogenized fetal lung using the Quantikine Mouse IL-1β Immunoassay (R&D Systems). IL-1β concentrations were normalized to total protein as measured by BCA assay (Pierce).

Tissue processing and immunolabeling

Mouse lung tissue, fetal lung explants, and cultured macrophages were fixed, processed, and immunolabeled using standard techniques. For immunofluorescence, Alexa-conjugated secondary Abs were used for visualization, and nuclei were alternatively labeled with DAPI or TO-PRO-3. Immunohistochemical processing was performed using Vectastain Kits and 3,3′-diaminobenzidine visualization (Vector Laboratories) with Mayer's H&E counterstaining (Sigma-Aldrich).

Imaging and image analysis

Confocal images were acquired using either an Olympus FV1000 (Olympus) or Leica SPE (Leica Microsystems) laser scanning confocal microscope. Widefield fluorescence images and brightfield images of fetal mouse lung explants were obtained using an Olympus IX81 microscope equipped with a Hamamatsu Orca ER CCD monochrome camera and Slidebook software (Olympus). Color images of lung specimens were photographed using a Nikon TE800 and SPOT color CCD camera (Diagnostic Instruments). All microscopy images were saved in the Tagged Image File format and imported into Photoshop (Adobe Systems) for processing. Images for comparison were always identically processed. For live imaging of NF-κB activation, NGL explants were cultured in a stage-top incubator (Okolab) and imaged using an Olympus IX81 inverted microscope (Olympus) with a WeatherStation enclosure. Exact temperature, humidity, and CO_2 concentration were maintained during the imaging experiment. Fluorescence images were acquired every 10 min for the first 2 h and then every 20 min for 2–24 h of culture. Time series images were processed in Slidebook (Olympus). Lung morphometery and cell counting were performed using the Image Processing Tool Kit (Reindeer Graphics) within Photoshop (Adobe Systems). Fractional lung volumes were measured by analyzing images from serial fetal lung sections using a counting grid function. The fractions of airspace, large airway epithelia, small or distal airway epithelia, and mesenchyme were measured on E-cadherin–labeled sections. Septal thickness in newborn lungs was measured using the global intercept function. To account for possible anisotropy, intercepts in each image were measured over multiple iterations with 10˚ of rotation between each measurement. The mean intercept length for each image was recorded.

Results

LPS activates NF-κB in fetal lung macrophages

Where LPS initially activates the innate immune system in fetal lungs has not been identified. We therefore investigated the localization and kinetics of LPS-induced NF-κB activation in E15 fetal lung explants from NF-κB transgenic reporter mouse (NGL), which expresses GFP and luciferase downstream of a promoter synthesized from the NF-κB–binding repeats within the HIV-1 long terminal repeat (20). Time-lapse imaging of NGL explants demonstrated NF-κB–dependent GFP expression by 90 min after LPS treatment, with continued GFP expression to 12 h (Fig. 1*A–D*, Supplemental Movies 1–4). GFP expression localized to cells throughout the lung mesenchyme. To visualize the cellular site of NF-κB–GFP expression at higher resolution, we imaged NGL explants using confocal microscopy. As seen in Fig. 1*E–M*, 2 h of LPS treatment stimulated GFP expression predominantly in cells that colabeled with the macrophage marker CD68. Following 12 h of LPS treatment, GFP reporter expression was detected both in CD68-positive macrophages and in adjacent mesenchymal cells (arrows in Fig. 1*G*, 1*M*). The close proximity of GFP-expressing mesenchymal cells to CD68-postive macrophages suggests release of secondary inflammatory mediators that could then activate NF-κB in nearby cells.

Because macrophages were present in E15 fetal lungs and positioned to regulate inflammatory responses, we examined the timing of macrophage appearance into the fetal mouse lung during development. Immunostaining identified CD68-positive cells in the lung mesenchyme as early as E10 during the initial steps of lung formation (Fig. 2*A*). Macrophages remained present in the mesenchyme throughout fetal development. Fetal lung macrophages also expressed F4/80 (Fig. 2*B*). To measure function, we tested if LPS could directly activate isolated fetal lung macrophages. We obtained macrophages from E15 lungs using anti-CD11b–coated magnetic beads (Fig. 2*C*), exposed them to *E. coli* LPS, and measured gene expression by RT-PCR. LPS stimulated macro-

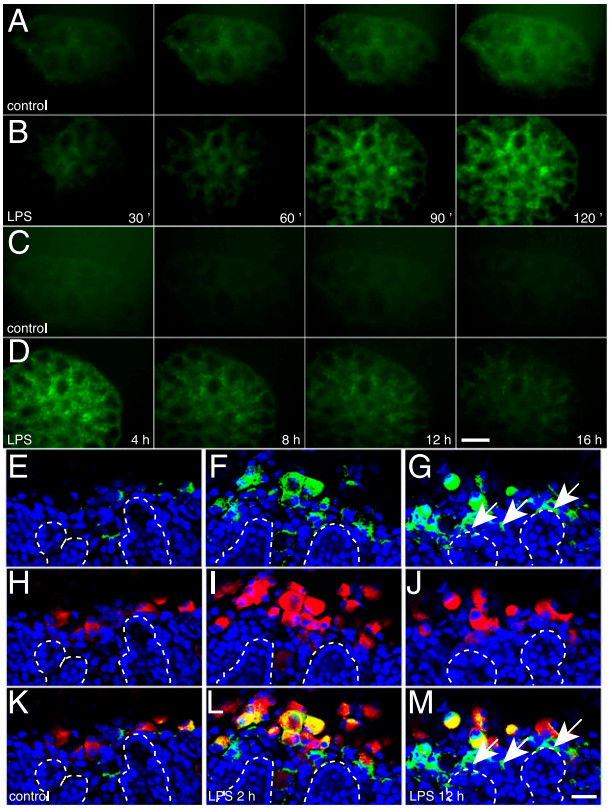

FIGURE 1. LPS stimulates NF-κB–dependent GFP expression in NGL fetal mouse lung explants. E15 fetal lung explants from NGL mice were cultured under control conditions (*A*, *C*) or in the presence of LPS (*B*, *D*) and imaged by time-lapse wide field fluorescence microscopy. Increased GFP expression was detected within 90 min of LPS treatment (*B*) and persisted beyond 12 h (*D*). Scale bar, 100 μm (*A–D*). Confocal images of control and LPS-treated NGL explants were obtained to better identify sites of GFP expression (*E–M*). Explants were fixed and immunostained for CD68 (red, *H–M*) following 2 and 12 h of LPS treatment. Nuclei were labeled with DAPI. In LPS-treated explants, NF-κB–GFP expression colocalized with CD68-postive macrophages following LPS treatment (GFP green, *E–G*; CD68 and GFP merged image in *K–M*). At 12 h, GFP expression was also detected in CD68-negative cells (arrows, *G*, *M*). Saccular airways are indicated by dotted lines. Scale bar, 25 μm (*E–M*).

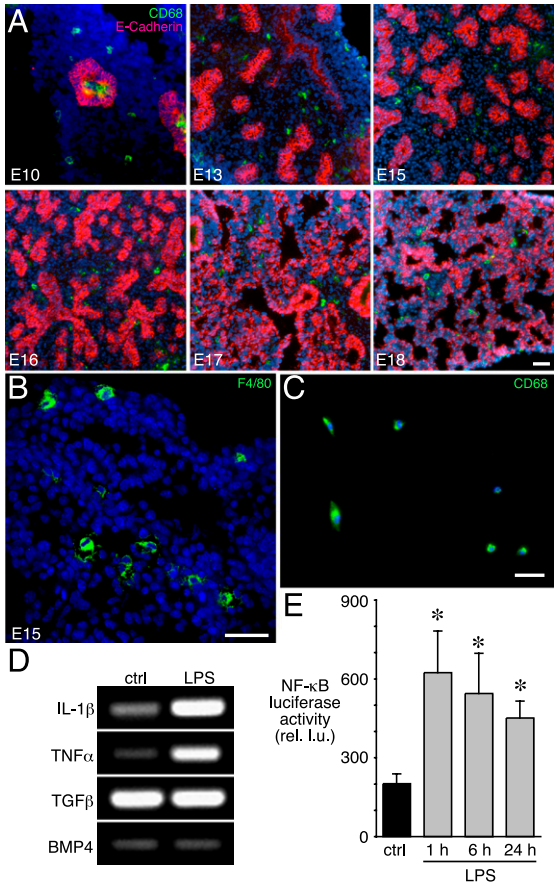

FIGURE 2. Macrophages are present in the fetal mouse lung and respond to LPS. *A*, Frozen sections of E10–E18 fetal mouse lungs were immunostained with Abs against the macrophage marker CD68 (green) and the epithelial marker E-cadherin (red). Nuclei were labeled with DAPI. Scale bar, 50 μm. *B*, Macrophages from E15 lung also express F4/80 (green). Scale bar, 50 μm. *C*, Fetal lung macrophages isolated by anti-CD11b magnetic bead separation from E15 lungs expressed CD68 (green). Scale bar, 50 μm. *D*, Macrophages were treated with *E. coli* LPS for 4 h, and gene expression was measured by RT-PCR. LPS increased IL-1β and TNF-α expression, but had no effect on TGF-β or BMP4. *E*, LPS activates NF-κB in E15 fetal mouse lung macrophages. Macrophages isolated from E15 NGL lungs were treated with LPS for the indicated times. NF-κB–luciferase was measured by luminometry. $*p < 0.05$; $n = 6$.

phage expression of the inflammatory mediators IL-1β and TNF-α, but did not affect expression of TGF-β or BMP4 (Fig. 2*D*). Using macrophages isolated from E15 NGL mouse lungs, we next showed that LPS directly activates NF-κB–dependent luciferase activity (Fig. 2*E*). These data clearly demonstrate that macrophages within the fetal mouse lung respond to LPS and can produce inflammatory mediators.

Macrophage activation inhibits saccular airway branching

We have previously developed an E15 fetal mouse lung explant model to study the mechanisms regulating canalicular and saccular stage airway branching (10, 16). Following 72 h of culture, the structures along the periphery of these explants resemble early saccular lungs by undergoing type I/type II cell differentiation, thinning of the mesenchyme, and branching of small airways. This model parallels the period of lung development occurring postnatally in extremely preterm infants born between 23 and 28 wk gestation, making it relevant for investigating BPD pathogenesis. Airway branching in E15 explants requires fibronectin, mesenchymal $\alpha_8\beta_1$-integrin expression, and fibroblast growth factor-10 (FGF-10) (10, 12, 13). We have also previously shown that TLR agonists, hyperoxia exposure, and tracheal aspirate fluid from preterm infants exposed to antenatal inflammation can each inhibit airway branching in cultured explants (10, 13, 22). To initially test if the inhibitory effects of LPS on branching required macrophage activation, we depleted macrophages from E15 fetal lung explants using clodronate-containing liposomes (Fig. 3). We then measured the number of new airways that formed along the periphery of each explant between 24 h and 72 h. Although LPS inhibited formation of new saccular airways in control and empty liposome-treated explants (Fig. 3*E*, 3*G*), clodronate depletion of macrophages protected saccular airway branching from the effects of LPS (Fig. 3*F*, 3*G*). Macrophage depletion also substantially reduced the amount of LPS-induced IL-1β within lung explants (Fig. 3*H*), suggesting macrophages produce most of the IL-1β within LPS-treated fetal lung explants. Macrophages, therefore, are important for both production of inflammatory mediators within the fetal lung and inhibiting airway branching following exposure to LPS.

As clodronate could have off-target toxic effects, we next used a molecular approach to test if NF-κB activation in macrophages was required for LPS-dependent disruption of saccular airway

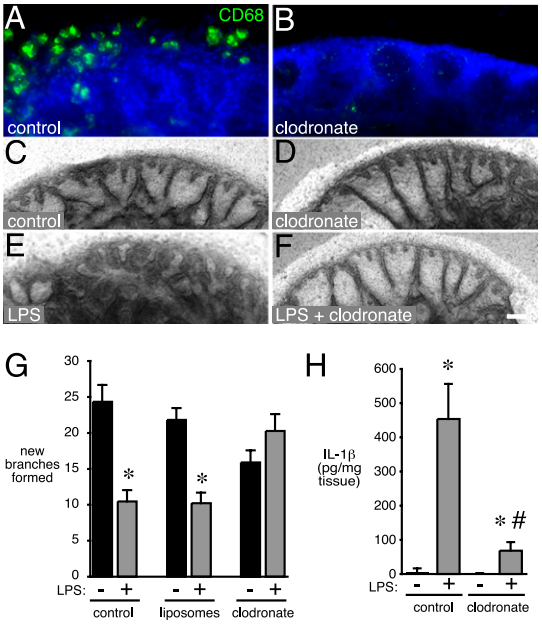

FIGURE 3. Macrophage depletion protects fetal lung explants from the effects of LPS. *A* and *B*, E15 fetal mouse lung explants were cultured in the absence or presence of liposomal clodronate (50 mg/ml). Following 72 h of culture, explants were immunostained with Abs against the macrophage marker CD68 to verify macrophage depletion (*B*). *C–F*, Brightfield images show that LPS inhibits formation of new saccular airway branches (*E*), but this effect is prevented in clodronate-treated explants (*F*). Scale bar, 50 μm (*A–F*). *G*, LPS inhibited formation of new saccular airways in control and empty liposome-treated explants ($*p < 0.001$; $n = 24$). However, LPS did not inhibit branching in clodronate-treated explants. *H*, Clodronate depletion of macrophages reduced the amount of IL-1β released following LPS treatment ($*p < 0.05$ LPS compared with untreated [$n = 4$], $^{\#}p < 0.01$ LPS compared with LPS + clodronate [$n = 4$]).

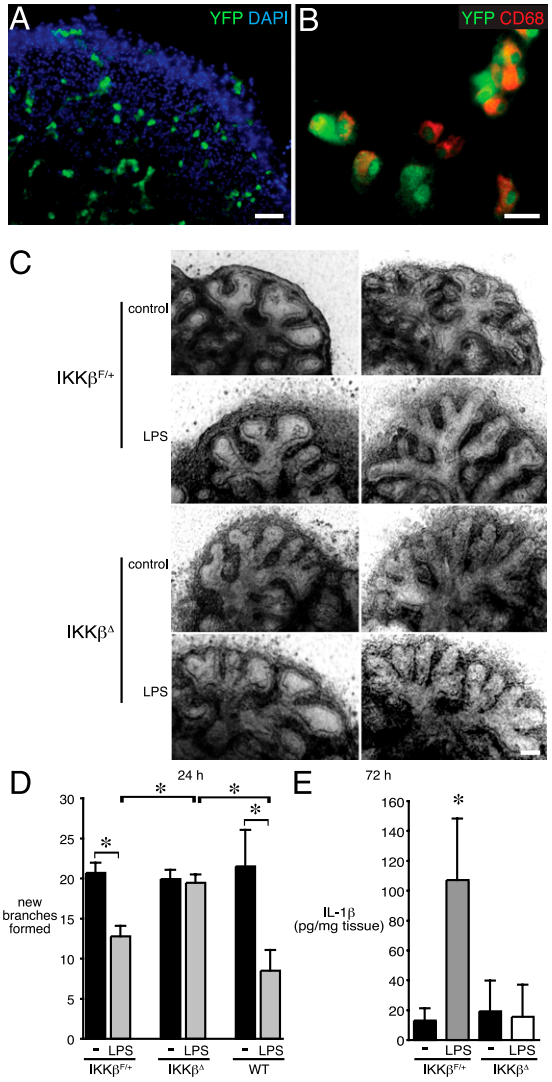

FIGURE 4. Targeted deletion of IKKβ in macrophages protects fetal lung explants from the effects of LPS. *A*, LysM-Cre recombinase activity in E15 fetal mouse lung explants. Fluorescence images of cultured LysM-Cre:Rosa26-YFP reporter explants. YFP expression is seen in macrophages throughout the explant. Cell nuclei visualized with DAPI. Scale bar, 50 μm. *B*, LysM-Cre:Rosa26-YFP macrophages immunostained with Ab against CD68 (red) to show overlapping expression. Scale bar, 10 μm. *C*, LPS does not inhibit saccular airway branching in IKKβΔ explants. Scale bar, 50 μm. *D*, LPS inhibited the number of new saccular airways that formed between 24 and 72 h of culture in $IKK\beta^{F/+}$ and wild-type BALB/cJ (WT) explants, but had no effect on branching in IKKβΔ explants ($*p < 0.05$; $n = 28$). *E*, Macrophage expression of IKKβ is required for normal IL-1β expression following LPS treatment. LPS increased IL-1β production in littermate control $IKK\beta^{F/+}$ explants ($*p < 0.05$; $n = 6$), but did not significantly increase IL-1β in IKKβΔ explants ($^{\#}p < 0.05$ compared with LPS in $IKK\beta^{F/+}$ explants; $n = 6$).

branching. For these experiments, we used mice with macrophage-specific IκB kinase β (IKKβ) deletion. LysM-Cre:$IKK\beta^{f/f}$ mice (IKKβΔ) lack functional IKKβ in myeloid cells, including macrophages and monocytes (21). LysM-Cre recombinase activity was confirmed in fetal lung explant macrophages using Rosa26-YFP reporter mice (Fig. 4*A*, 4*B*). We next measured the effects of LPS on explants from IKKβΔ and littermate controls. LPS failed to inhibit saccular airway branching in IKKβΔ explants (Fig. 4*C*, 4*D*), supporting the critical role of macrophages in inflammation-dependent disruption of airway morphogenesis and identifying NF-κB as the operative signaling pathway in mediating this effect. The total amount of IL-1β produced in LPS-treated IKKβΔ explants was much lower than in explants from littermate controls, again demonstrating that macrophages are responsible for a majority of the IL-1β produced in the LPS-treated fetal lung (Fig. 4*E*).

Having observed that activation of the NF-κB pathway in macrophages appears to mediate the effects of LPS on saccular airway morphogenesis, we next tested if NF-κB activation in macrophages is sufficient to disrupt airway morphogenesis and whether macrophages can impact airway formation in vivo. For these experiments, we used IKFM transgenic mice that express a macrophage-specific doxycycline-inducible *c-fms* transactivator and a constitutively active IKKβ mutant (cIKKβ) gene downstream of a *tet*-responsive promoter (L. Connelly et al., submitted for publication). We cultured saccular stage fetal lung explants from IKFM mice and control littermates in the absence or presence of doxycycline (Fig. 5*A*, 5*B*). Doxycycline had no effect on branching in control explants, but caused airway dilation and reduced branch formation in IKFM explants (Fig. 5*B*). Excessive IKKβ activity in IKFM macrophages inhibited branching, as did adding LPS (Fig. 5*C*). Inducing cIKKβ expression in macrophages increased IL-1β expression in fetal lung explants, demonstrating activity of the transgene (Fig. 5*D*). These results suggest that NF-κB activation specifically in macrophages is sufficient to disrupt normal fetal lung morphogenesis.

Targeted NF-κB activation in mouse macrophages disrupts lung morphogenesis

We next tested if macrophage-specific overexpression of cIKKβ in IKFM mice could alter lung morphogenesis in intact fetal mice.

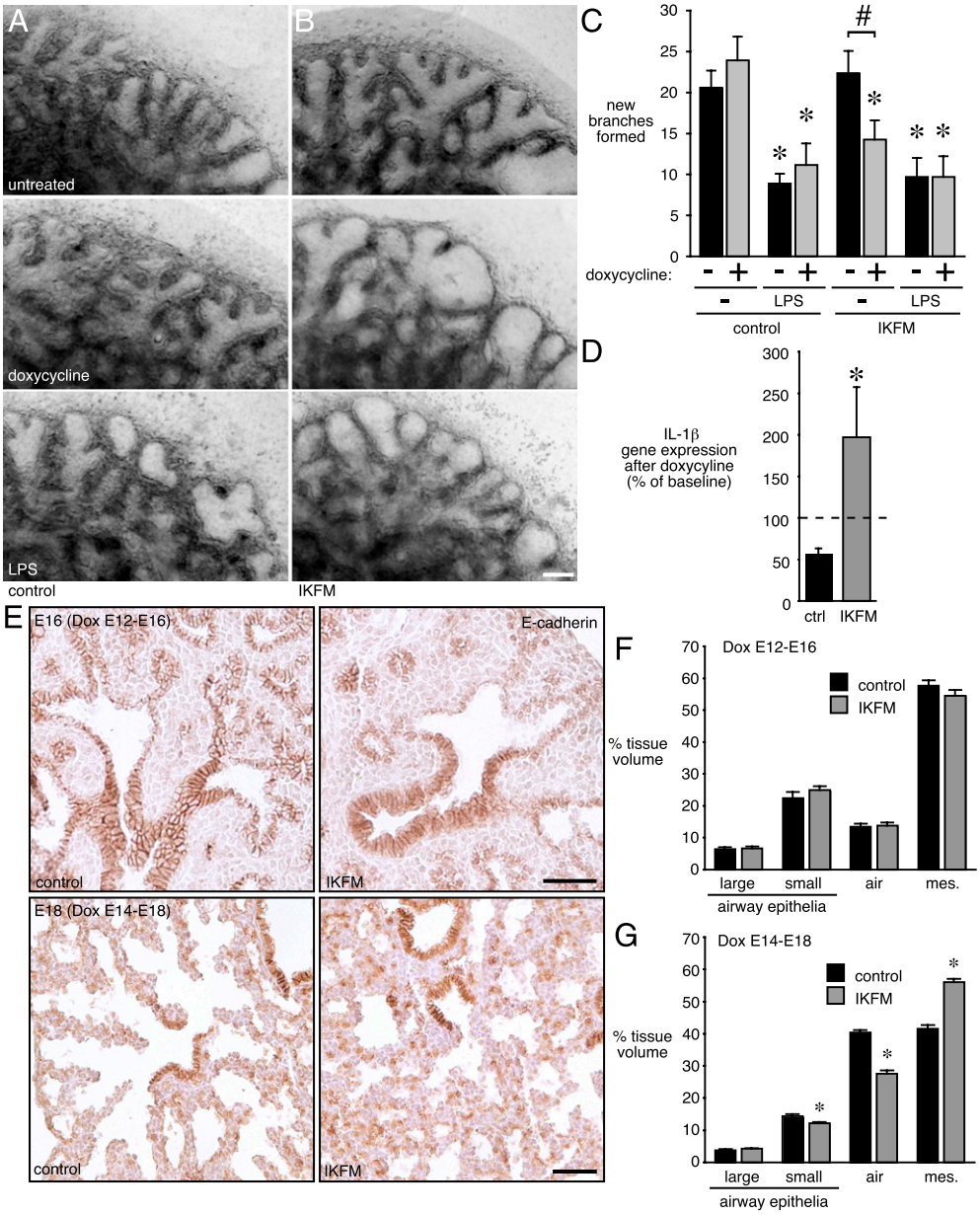

FIGURE 5. IKKβ activity in macrophages is sufficient to inhibit saccular airway branching. Brightfield images of E15 fetal lung explants from IKFM mice (*B*) and littermate controls (*A*) cultured under control conditions (*top panels*), in the presence of doxycycline (*middle panels*), and in the presence of LPS (*bottom panels*). Scale bar, 50 μm (*A*, *B*). *C*, Doxycycline induction if cIKKβ in macrophages inhibited saccular airway branching. Doxycycline had no effect in littermate control explants, whereas LPS inhibited formation of new saccular airway branches in both control and IKFM explants ($*p < 0.05$ compared with branches formed in the absence of doxycycline and without LPS [$n = 9$], $\#p < 0.05$ compared with IKFM explants in the absence of doxycycline and without LPS [$n = 9$]). *D*, Doxycycline induction of cIKKβ in macrophages increased IL-1β expression in IKFM explants ($*p < 0.05$; $n = 9$). Dotted line indicates baseline expression level. *E*, Overexpression of cIKKβ in macrophages inhibits saccular stage lung morphogenesis in vivo. IKFM mice were given doxycycline (Dox) from either E12–E16 (*top panels*) or E14–E18 (*bottom panels*). Sections were immunostained using anti–E-cadherin to label epithelia. Scale bars, 100 μm. Lung morphogenesis did not appear altered in mice given Dox from E12–E16, either by histology or morphometric measurement of large and small airway epithelia, airspace (air), and mesenchymal (mes.) volumes (*F*). Dox administration from E14–E18 disrupted normal lung development, with IKFM lungs having smaller airways with reduced branching and expansion (*E*, *G*). Morphometry measurements confirmed decreased airspace and increased mesenchymal volumes in IKFM mice treated with Dox (*G*; $*p < 0.001$; $n = 27$).

Pregnant IKFM mice were treated with doxycycline to activate macrophages during either the late pseudoglandular stage (E12–E16) or from the late pseudoglandular stage through the canalicular and early saccular stages (E14–E18, Fig. 5*E*). Doxycycline administration from E12–E16 did not cause apparent changes in airway formation (Fig. 5*E*, 5*F*). However, transgene activation from E14–E18 caused significant changes with less airspace and increased mesenchyme in IKFM lungs compared with littermate controls (Fig. 5*E*, 5*G*). These differences were consistent with defects in saccular airway branching morphogenesis. The lack of effect in mice treated E12–E16 suggests that airway branching in the E14–E18 lung may have a window of vulnerability to macrophage activation. These data support the idea that macrophage activation and subsequent lung inflammation disrupt the later stages of airway formation.

To investigate how the morphological changes observed in IKFM mice affect respiratory function, mice treated with doxycycline from E14–E18 were allowed to deliver at E19 and E20.

Disruption of normal lung development in IKFM pups led to reduced survival in the first 24 h. Newborn IKFM mice appeared cyanotic, and many died soon after birth, whereas control littermates appeared healthy (Fig. 6*A*, 6*B*). Histological examination of newborn IKFM lungs again showed a thickened lung interstitium compared with control littermates (Fig. 6*C*, 6*D*). As with mice harvested at E18, the microscopic appearance of newborn IKFM mouse lungs, with thickened interstitium and simplified airways, showed similarities to the lungs of patients with BPD. Macrophages were present both lining the airway lumen and within the interstitium in both control and IKFM newborn lungs (Fig. 6*E*). IKFM mice had increased numbers of F4/80-positive cells, which may represent increased macrophage recruitment, maturation, or proliferation (Fig. 6*F*). IKFM and control lungs contained similar numbers of lymphocytes and neutrophils (Fig. 6*G*), without signs of consolidated infiltrates or edema. These data further demonstrate that macrophage NF-κB activation, which could occur secondary to infection or other insults, can inhibit saccular airway morphogenesis.

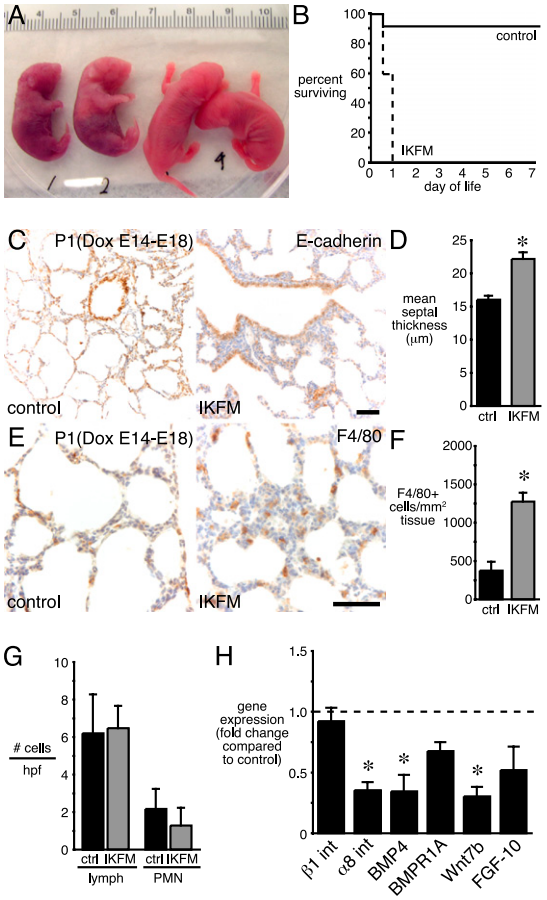

FIGURE 6. Targeted expression of a cIKKβ in fetal macrophages causes arrested lung development and perinatal lethality. *A* and *B*, Pregnant mice were treated with doxycycline from E14–E18 and then allowed to deliver. Newborn IKFM mice were born alive but developed respiratory distress and became cyanotic and lethargic soon after delivery. Littermate controls appeared healthy and vigorous. *C* and *D*, Newborn IKFM lungs have abnormal structure, with wider interstitium between airways and increased mean septal thickness ($*p < 0.01$; $\nu = 15$). Scale bar, 100 μm (*C*, *D*). *E* and *F*, Immunostaining for F4/80 shows increased numbers of macrophages in newborn IKFM lungs compared with control littermates. Scale bar, 100 μm (*E*, *F*). *G*, The numbers of lymphocytes and neutrophils (PMN) in the lungs of newborn IKFM mice and littermate controls were similar. *H*, Reduced expression of genes required for normal branching morphogenesis in newborn IKFM lungs treated from E14–E18 with doxycycline. Expression measured by real-time PCR ($*p < 0.05$; $n = 7$). Dotted line indicates control expression level.

Macrophage activation from E14–E18 in IKFM mice caused a persistent inhibition of expression of multiple genes critical for branching morphogenesis in newborn lungs (12, 23, 24), including reduced expression of the α_8 integrin subunit, BMP4, and Wnt7b (Fig. 6*H*). Expression of BMPR1A and FGF-10 also trended lower in IKFM lungs. Macrophage activation and release of inflammatory cytokines can therefore inhibit gene expression in the developing lung, leading to altered airway morphogenesis. These findings are consistent with our findings in lung explants, where macrophage activation can inhibit airway branching in the absence of systemic circulation. Activation of NF-κB in fetal lung macrophages could therefore be a common feature of insults that disrupt normal airway morphogenesis. As such, our model of a BPD-like phenotype in IKFM mice may be useful in further defining the pathogenesis and course of BPD.

Discussion

In this study, we demonstrate that NF-κB activation in macrophages is a key initial step in the fetal lung inflammatory response and sufficient to disrupt fetal lung morphogenesis. Macrophages in the canalicular or saccular stage fetal lung reside in the interstitium and respond to endotoxin. The NF-κB–dependent release of inflammatory mediators from these activated macrophages may then cause a second wave of signaling in neighboring cells, including the mesenchymal cells critical for airway morphogenesis. Even when the entire fetal lung is exposed to LPS, as is the case when explants are treated with LPS, macrophages appear to be the major cellular site of NF-κB activation and cytokine production. Macrophage depletion or targeted IKKβ deletion dramatically reduced the amount of IL-1β produced in response to LPS treatment and protected airway branching from the inhibitory effects of LPS. In addition, targeted activation of fetal lung macrophages was sufficient to disrupt lung morphogenesis, causing perinatal lethality and airway pathology that resembles human BPD.

These findings fill an important gap in our knowledge of how the immature fetal lung responds to inflammatory stimuli. When preterm infants are exposed to chorioamnionitis in utero, inflammatory cytokines accumulate in their airways (9). The infants with high levels of inflammatory mediators in their lungs at birth are more likely to develop BPD (25). Not only are macrophages the major source of inflammatory mediators in the lung, but also their location in the fetal lung interstitium may increase the likelihood that macrophage-derived cytokines can affect immediately adjacent cells. Recent studies have demonstrated increased macrophage recruitment to fetal or newborn lungs following either mechanical or endotoxin-mediated injury (26, 27). However, our current study is the first to connect macrophage activation and altered lung morphogenesis, to our knowledge. We propose a two-wave mechanism for NF-κB activation leading to arrested lung development in BPD. In this model, microbial products initially activate NF-κB in lung macrophages. The release of inflammatory mediators, particularly IL-1β and/or TNF-α, then causes NF-κB activation in the adjacent mesenchymal cells. NF-κB activation in the mesenchyme disrupts expression of genes important for the precise, controlled epithelial–mesenchymal interactions that regulate airway branching. This mechanism is supported by our previous findings that NF-κB activation in fetal lung mesenchymal cells interferes with normal expression of important developmental genes, including FGF-10 and integrin $\alpha_8\beta_1$ (9, 12–14). The decreased BMP4 expression in IKFM lungs may be due

to the direct effect of inflammatory cytokines on the airway epithelium (28) or secondary to reduced FGF-10 expression in the mesenchyme (23). Although inflammatory mediators that signal via other pathways may also affect lung development, those that can activate NF-κB in target cells appear to be most detrimental.

The IFKM mouse strain may provide an important model for further studying how macrophage activation and inflammation arrests lung development, particularly if the phenotype can be modulated so that affected pups can survive the neonatal period. The inducible cIKKβ transgene allows macrophage activation at distinct stages of lung development, as compared with postnatal rodent models that are restricted to studying the late saccular and alveolar stages of lung development (29). Human infants born at a comparable stage of lung development to that of newborn mice very rarely develop BPD, making these experimental models less useful for investigating the early mechanisms of BPD pathogenesis (3). IKFM mice may also allow us to test if the effects of macrophage activation are reversible or persistent, how repetitive activations affect lung development, and if macrophage activation alters the susceptibility to other types of injury including hyperoxia, mechanical trauma, and viral infection. These future studies may help us better understand why some infants develop only mild BPD and others have more severe or progressive disease. The IKFM experimental model will potentially permit studies that target different phases of the inflammatory response in the fetal and newborn lung to better identify potential strategies for treatment.

Although fetal lung macrophages clearly respond to innate immune stimuli, their functional role in normal embryogenesis remains uncertain. In developing tissues, macrophages may remove cellular debris, remodel extracellular matrix, or express growth factors (30). Removal of apoptotic cells may be critical for lung morphogenesis, as at least one study has demonstrated that mice lacking the phosphoserine receptor are unable to phagocytose apoptotic cells and die following birth with abnormal lung structure (31). In the developing mammary gland, macrophages localize to collagen fibrils along elongating ductal branches, possibly playing a role in extracellular matrix remodeling (32). Macrophages present in the fetal kidney may contribute to development by expressing specific Wnt ligands (33). We do not yet know if fetal lung macrophages play a similar trophic role in normal airway morphogenesis. In addition to the downstream effects of macrophage-derived cytokines on mesenchymal cell gene expression, inflammatory activation could divert macrophages from their yet uncharacterized developmental or trophic roles. This intersection of inflammatory and developmental pathways could therefore be a focal point for disease pathogenesis.

The two-wave model for propagation of inflammatory signals that disrupt branching morphogenesis suggests several potential therapeutic strategies for preventing BPD. Targeting macrophage activation could prevent the initial wave of fetal lung inflammation. The feasibility of this approach is supported by our experimental data using macrophage depletion and targeted deletion of IKKβ. However, many women clinically present already in preterm labor and with evidence of chorioamnionitis (34). In these situations, fetal lung macrophage activation may have occurred prior to delivery. Therefore, alternative strategies could target inflammatory mediators such as IL-1β and TNF-α to prevent the effects of inflammation on mesenchymal gene expression and altered epithelial–mesenchymal interactions. Finally, approaches that restore the mesenchymal cell phenotype to a normal fetal lung gene expression pattern and cell behavior could promote ongoing lung morphogenesis even in preterm infants with previous inflammatory exposures.

Acknowledgments

We thank Dr. Michael Karin for the LysM-Cre:IKKβ$^{F/F}$ mice. We also thank Riet van der Meer, Li Zhang, Amanda Stinnett, Kassidy Thibodeau, and Lianyi Chen for assistance and scientific colleagues for helpful advice and comments.

Disclosures

The authors have no financial conflicts of interest.

References

1. Warburton, D., M. Schwarz, D. Tefft, G. Flores-Delgado, K. D. Anderson, and W. V. Cardoso. 2000. The molecular basis of lung morphogenesis. *Mech. Dev.* 92: 55–81.
2. Metzger, R. J., O. D. Klein, G. R. Martin, and M. A. Krasnow. 2008. The branching programme of mouse lung development. *Nature* 453: 745–750.
3. Stoll, B. J., N. I. Hansen, E. F. Bell, S. Shankaran, A. R. Laptook, M. C. Walsh, E. C. Hale, N. S. Newman, K. Schibler, W. A. Carlo, et al; Eunice Kennedy Shriver National Institute of Child Health and Human Development Neonatal Research Network. 2010. Neonatal outcomes of extremely preterm infants from the NICHD Neonatal Research Network. *Pediatrics* 126: 443–456.
4. May, C., M. Prendergast, S. Salman, G. F. Rafferty, and A. Greenough. 2009. Chest radiograph thoracic areas and lung volumes in infants developing bronchopulmonary dysplasia. *Pediatr. Pulmonol.* 44: 80–85.
5. Bhandari, A., and V. Bhandari. 2009. Pitfalls, problems, and progress in bronchopulmonary dysplasia. *Pediatrics* 123: 1562–1573.
6. Baraldi, E., and M. Filippone. 2007. Chronic lung disease after premature birth. *N. Engl. J. Med.* 357: 1946–1955.
7. Lahra, M. M., P. J. Beeby, and H. E. Jeffery. 2009. Intrauterine inflammation, neonatal sepsis, and chronic lung disease: a 13-year hospital cohort study. *Pediatrics* 123: 1314–1319.
8. Paananen, R., A. K. Husa, R. Vuolteenaho, R. Herva, T. Kaukola, and M. Hallman. 2009. Blood cytokines during the perinatal period in very preterm infants: relationship of inflammatory response and bronchopulmonary dysplasia. *J. Pediatr.* 154: 39–43.e3.
9. Benjamin, J. T., B. J. Carver, E. J. Plosa, Y. Yamamoto, J. D. Miller, J. H. Liu, R. van der Meer, T. S. Blackwell, and L. S. Prince. 2010. NF-kappaB activation limits airway branching through inhibition of Sp1-mediated fibroblast growth factor-10 expression. *J. Immunol.* 185: 4896–4903.
10. Prince, L. S., H. I. Dieperink, V. O. Okoh, G. A. Fierro-Perez, and R. L. Lallone. 2005. Toll-like receptor signaling inhibits structural development of the distal fetal mouse lung. *Dev. Dyn.* 233: 553–561.
11. Willet, K. E., A. H. Jobe, M. Ikegami, J. Newnham, S. Brennan, and P. D. Sly. 2000. Antenatal endotoxin and glucocorticoid effects on lung morphometry in preterm lambs. *Pediatr. Res.* 48: 782–788.
12. Benjamin, J. T., D. C. Gaston, B. A. Halloran, L. M. Schnapp, R. Zent, and L. S. Prince. 2009. The role of integrin alpha8beta1 in fetal lung morphogenesis and injury. *Dev. Biol.* 335: 407–417.
13. Benjamin, J. T., R. J. Smith, B. A. Halloran, T. J. Day, D. R. Kelly, and L. S. Prince. 2007. FGF-10 is decreased in bronchopulmonary dysplasia and suppressed by Toll-like receptor activation. *Am. J. Physiol. Lung Cell. Mol. Physiol.* 292: L550–L558.
14. Miller, J. D., J. T. Benjamin, D. R. Kelly, D. B. Frank, and L. S. Prince. 2010. Chorioamnionitis stimulates angiogenesis in saccular stage fetal lungs via CC chemokines. *Am. J. Physiol. Lung Cell. Mol. Physiol.* 298: L637–L645.
15. Andonegui, G., C. S. Bonder, F. Green, S. C. Mullaly, L. Zbytnuik, E. Raharjo, and P. Kubes. 2003. Endothelium-derived Toll-like receptor-4 is the key molecule in LPS-induced neutrophil sequestration into lungs. *J. Clin. Invest.* 111: 1011–1020.
16. Prince, L. S., V. O. Okoh, T. O. Moninger, and S. Matalon. 2004. Lipopolysaccharide increases alveolar type II cell number in fetal mouse lungs through Toll-like receptor 4 and NF-kappaB. *Am. J. Physiol. Lung Cell. Mol. Physiol.* 287: L999–L1006.
17. Henson, P. M., and D. A. Hume. 2006. Apoptotic cell removal in development and tissue homeostasis. *Trends Immunol.* 27: 244–250.
18. Hopkinson-Woolley, J., D. Hughes, S. Gordon, and P. Martin. 1994. Macrophage recruitment during limb development and wound healing in the embryonic and foetal mouse. *J. Cell Sci.* 107: 1159–1167.
19. Tomlinson, M. L., C. Garcia-Morales, M. Abu-Elmagd, and G. N. Wheeler. 2008. Three matrix metalloproteinases are required in vivo for macrophage migration during embryonic development. *Mech. Dev.* 125: 1059–1070.
20. Everhart, M. B., W. Han, T. P. Sherrill, M. Arutiunov, V. V. Polosukhin, J. R. Burke, R. T. Sadikot, J. W. Christman, F. E. Yull, and T. S. Blackwell. 2006. Duration and intensity of NF-kappaB activity determine the severity of endotoxin-induced acute lung injury. *J. Immunol.* 176: 4995–5005.
21. Greten, F. R., L. Eckmann, T. F. Greten, J. M. Park, Z. W. Li, L. J. Egan, M. F. Kagnoff, and M. Karin. 2004. IKKbeta links inflammation and tumorigenesis in a mouse model of colitis-associated cancer. *Cell* 118: 285–296.
22. Dieperink, H. I., T. S. Blackwell, and L. S. Prince. 2006. Hyperoxia and apoptosis in developing mouse lung mesenchyme. *Pediatr. Res.* 59: 185–190.
23. Weaver, M., N. R. Dunn, and B. L. Hogan. 2000. Bmp4 and Fgf10 play opposing roles during lung bud morphogenesis. *Development* 127: 2695–2704.
24. Rajagopal, J., T. J. Carroll, J. S. Guseh, S. A. Bores, L. J. Blank, W. J. Anderson, J. Yu, Q. Zhou, A. P. McMahon, and D. A. Melton. 2008. Wnt7b stimulates

embryonic lung growth by coordinately increasing the replication of epithelium and mesenchyme. *Development* 135: 1625–1634.
25. Choi, C. W., B. I. Kim, H. S. Kim, J. D. Park, J. H. Choi, and D. W. Son. 2006. Increase of interleukin-6 in tracheal aspirate at birth: a predictor of subsequent bronchopulmonary dysplasia in preterm infants. *Acta Paediatr.* 95: 38–43.
26. Hillman, N. H., G. R. Polglase, J. J. Pillow, M. Saito, S. G. Kallapur, and A. H. Jobe. 2011. Inflammation and lung maturation from stretch injury in preterm fetal sheep. *Am. J. Physiol. Lung Cell. Mol. Physiol.* 300: L232–L241.
27. Cao, L., J. Wang, I. Tseu, D. Luo, and M. Post. 2009. Maternal exposure to endotoxin delays alveolarization during postnatal rat lung development. *Am. J. Physiol. Lung Cell. Mol. Physiol.* 296: L726–L737.
28. Zhu, N. L., C. Li, H. H. Huang, M. Sebald, V. A. Londhe, N. Heisterkamp, D. Warburton, S. Bellusci, and P. Minoo. 2007. TNF-alpha represses transcription of human Bone Morphogenetic Protein-4 in lung epithelial cells. *Gene* 393: 70–80.
29. McGrath-Morrow, S. A., and J. Stahl. 2001. Apoptosis in neonatal murine lung exposed to hyperoxia. *Am. J. Respir. Cell Mol. Biol.* 25: 150–155.
30. Ovchinnikov, D. A. 2008. Macrophages in the embryo and beyond: much more than just giant phagocytes. *Genesis* 46: 447–462.
31. Li, M. O., M. R. Sarkisian, W. Z. Mehal, P. Rakic, and R. A. Flavell. 2003. Phosphatidylserine receptor is required for clearance of apoptotic cells. *Science* 302: 1560–1563.
32. Ingman, W. V., J. Wyckoff, V. Gouon-Evans, J. Condeelis, and J. W. Pollard. 2006. Macrophages promote collagen fibrillogenesis around terminal end buds of the developing mammary gland. *Dev. Dyn.* 235: 3222–3229.
33. Lin, S. L., B. Li, S. Rao, E. J. Yeo, T. E. Hudson, B. T. Nowlin, H. Pei, L. Chen, J. J. Zheng, T. J. Carroll, et al. 2010. Macrophage Wnt7b is critical for kidney repair and regeneration. *Proc. Natl. Acad. Sci. USA* 107: 4194–4199.
34. Romero, R., J. Espinoza, L. F. Gonçalves, J. P. Kusanovic, L. Friel, and S. Hassan. 2007. The role of inflammation and infection in preterm birth. *Semin. Reprod. Med.* 25: 21–39.